

**FORMATION KINETICS OF NITRIC OXIDE OF BIODIESEL RELATIVE TO
PETROLEUM DIESEL UNDER COMPARABLE OXYGEN EQUIVALENCE
RATIO IN A HOMOGENEOUS REACTOR**

A Thesis

by

GURLOVLEEN K. RATHORE

Submitted to the Office of Graduate Studies of
Texas A&M University
in partial fulfillment of the requirements for the degree of
MASTER OF SCIENCE

August 2010

Major Subject: Mechanical Engineering

**FORMATION KINETICS OF NITRIC OXIDE OF BIODIESEL RELATIVE TO
PETROLEUM DIESEL UNDER COMPARABLE OXYGEN EQUIVALENCE
RATIO IN A HOMOGENEOUS REACTOR**

A Thesis

by

GURLOVLEEN K. RATHORE

Submitted to the Office of Graduate Studies of
Texas A&M University
in partial fulfillment of the requirements for the degree of

MASTER OF SCIENCE

Approved by:

Co- Chairs of Committee,	Timothy J. Jacobs
	K. R. Rajagopal
Committee Members,	Jerald A. Caton
	Jay Walton
	Debra Fowler
Head of Department,	Dennis O' Neal

August 2010

Major Subject: Mechanical Engineering

ABSTRACT

Formation Kinetics of Nitric Oxide of Biodiesel Relative to Petroleum Diesel under Comparable Oxygen Equivalence Ratio in a Homogeneous Reactor. (August 2010)

Gurlovleen K. Rathore, B.S., University of Michigan, Ann Arbor

Co-Chairs of Advisory Committee: Dr. Timothy J. Jacobs
Dr. K. R. Rajagopal

Interest in biodiesel has piqued with advent of stringent emissions regulations. Biodiesel is a viable substitute for petroleum diesel because biodiesel produces significantly lower particulate and soot emissions relative to petroleum diesel. Higher nitric oxide (NO) emissions for biodiesel, however, are of primary concern in biodiesel-fueled engines. Search for an in-cylinder technique to reduce NO emissions for biodiesel has motivated studies to gain an improved understanding of fundamental factors that drive increase in NO emissions with biodiesel. Potential factors include fuel-bound oxygen, fuel-bound nitrogen and post-flame gas temperature. The role of fuel-bound oxygen however is debated in the literature. The research objective of this study is to computationally determine if biodiesel and petroleum diesel yield equivalent concentrations of NO with the same oxygen equivalence ratio in a 0-D homogeneous reactor, to explain the role of fuel-bound oxygen in biodiesel on increases in NO emissions with biodiesel.

The results from this study indicate that the biodiesel surrogate yields higher NO emissions than the n-heptane because of its lower oxygen consumption efficiency. The

lower oxygen consumption efficiency for biodiesel is likely because of the slower decomposition of the individual components and the blending ratios of the biodiesel surrogate blend. The relative differences in combustion efficiency of individual components of the biodiesel blend suggest this conclusion. The more efficient burning of the methyl esters relative to the n-heptane in biodiesel surrogate perhaps indicates the favorable role of fuel-bound oxygen in the fuel's combustion. The low utilization of oxygen by the biodiesel surrogate could not be explained in this study. The dominance of $\text{NO}_2 + \text{H} \leftrightarrow \text{NO} + \text{OH}$ and $\text{N} + \text{NO} \leftrightarrow \text{N}_2 + \text{O}$ mechanisms during biodiesel combustion however explain the high NO emissions for the biodiesel surrogate relative to the n-heptane. The biodiesel may yield lower NO emissions than the petroleum diesel if the blending ratios for the biodiesel are adjusted such that combustion efficiency of biodiesel and petroleum diesel is same or the $\text{NO}_2 + \text{H} \leftrightarrow \text{NO} + \text{OH}$ and $\text{N} + \text{NO} \leftrightarrow \text{N}_2 + \text{O}$ mechanisms are suppressed during biodiesel combustion.

DEDICATION

To my teachers

ACKNOWLEDGEMENTS

I thank my committee co-chairs, Dr. Timothy J. Jacobs and Dr. K. R. Rajagopal, and my committee members, Dr. Jerald A. Caton and Dr. Jay Walton, for their guidance and support throughout the course of this research. I also thank Dr. Chandrika Rajagopal and Dr. Debra Fowler for their encouragement during my years at Texas A&M University. Without their excellent mentoring and unconditional support, my time at Texas A&M would not have been as rewarding as it has been.

I also express my gratitude to my colleagues for their support and for financial support from State of Texas through grants from the Texas Environmental Research Consortium with funding provided by the Texas Commission on Environmental Quality and the Norman Hackerman Advanced Research Program. Finally, many thanks are due to my parents, Malkiat and Jasvir Rathore, my sisters, Maanjot and Babandeep Rathore, and my best friend, Meera Alagaraja, for their encouragement and unwavering love and support.

TABLE OF CONTENTS

	Page
ABSTRACT	iii
DEDICATION	v
ACKNOWLEDGEMENTS	vi
TABLE OF CONTENTS	vii
LIST OF FIGURES	ix
LIST OF TABLES	xi
1. INTRODUCTION AND LITERATURE REVIEW	1
1.1 Motivation	1
1.2 Background	1
1.3 Objective	3
2. NUMERICAL MODELING	11
2.1 Zero-Dimensional (0-D) Homogeneous Reactor	11
2.2 Fuel and NO _x Chemistry	14
2.3 Initial Conditions and Model Verification	15
2.3.1 Initial Conditions for the 0-D Homogeneous Reactor	15
2.3.1.1 Equivalence Ratio Calculation	15
2.3.1.2 Initial Mole Fractions Calculation	18
2.3.2 Model Verification	18
2.4 Data Collection	20
3. RESULTS AND DISCUSSION	21
3.1 Model Verification	21
3.2 Numerical Modeling	27
3.3 Limitations and Recommendations	39

	Page
4. SUMMARY AND CONCLUSIONS.....	42
4.1 Summary	42
4.2 Conclusions	45
REFERENCES.....	48
VITA	50

LIST OF FIGURES

FIGURE	Page
1 Comparison between computed values from a homogeneous reactor (HOMO) and equilibrium reactor (EQUIL) in CHEMKIN PRO for (a) temperature (K), (b) NO (ppm), (c) NO ₂ (ppm), and (d) O ₂ (ppm) as a function of oxygen equivalence ratio for n-heptane in a zero-dimensional constant pressure reactor with initial temperature and pressure at 886 K and 60 bars respectively, at residence reactor time = 20 seconds.....	22
2 Comparison between computed values from equilibrium reactor (EQUIL) in CHEMKIN-PRO and Adiabatic Flame Temperature Program (AFTP) for (a) temperature (K), (b) NO (ppm), (c) NO ₂ (ppm), and (d) O ₂ (ppm) as a function of oxygen equivalence ratio for n-heptane in a zero-dimensional constant pressure reactor with initial temperature and pressure at 886 K and 60 bars respectively.....	23
3 Comparison between computed values from a homogeneous reactor (HOMO) and equilibrium reactor (EQUIL) in CHEMKIN PRO for (a) temperature (K), (b) NO (ppm), (c) NO ₂ (ppm), and (d) O ₂ (ppm) as a function of oxygen equivalence ratio for a biodiesel surrogate in a zero-dimensional constant pressure reactor with initial temperature and pressure at 886 K and 60 bars respectively, at residence reactor time = 0.006, 1, and 3 seconds.....	25
4 Comparison of trends for computed temperature and oxygen as a function of reactor residence time in a zero-dimensional constant pressure homogenous reactor between initial conditions of our study ($T_i = 886$ K, $P_i = 60$ bars, $\phi = 1.0$) and five initial conditions selected from the ranges specified in [21] for which the biodiesel surrogate mechanisms have been experimentally validated in [21].....	26
5 Computed NO, NO ₂ and NO _x as a function of reactor residence time in a zero-dimensional constant pressure homogeneous reactor at initial temperature and pressure of 886 K and 60 bars respectively for n-heptane and the biodiesel surrogate	28

FIGURE	Page
6 Computed NO and NO _x on a dry basis as a function of reactor residence time in a zero-dimensional constant pressure homogeneous reactor at initial temperature and pressure of 886 K and 60 bars respectively for n-heptane and the biodiesel surrogate.....	29
7 Computed thermal NO and non-thermal NO contribution to total NO as a function of reactor residence time in a zero-dimensional constant pressure homogeneous reactor at initial temperature and pressure of 886 K and 60 bars respectively for n-heptane and the biodiesel surrogate.....	30
8 Computed temperature and oxygen as a function of reactor residence time in a zero-dimensional constant pressure homogeneous reactor at initial temperature and pressure of 886 K and 60 bars respectively for n-heptane and the biodiesel surrogate	32
9 Molar fuel conversion as a function of reactor residence time in a zero-dimensional constant pressure homogeneous reactor at initial temperature and pressure of 886 K and 60 bars respectively for n-heptane and the fuel components of the biodiesel surrogate.....	33
10 Absolute rate of production of NO for the dominant NO formation mechanisms at nominal 2000 ppmvd.....	35
11 Absolute rate of production of NO for the dominant NO formation mechanisms at nominal 4000 ppmvd.....	36
12 Absolute rate of production of NO for the dominant NO formation mechanisms at nominal 6000 ppmvd.....	37
13 Absolute rate of production of NO for the dominant NO formation mechanisms at reactor residence time of 0.003571 seconds.....	38

LIST OF TABLES

TABLE	Page
1 Comparison cases for oxygenated and non-oxygenated fuels under comparable oxygen environments	5
2 Initial conditions for Biodiesel and Petroleum Diesel	19
3 Total rate of production of NO at select NO values for the n-heptane and the biodiesel surrogate.....	34

1. INTRODUCTION AND LITERATURE REVIEW

1.1 Motivation

Interest in bio-derived fuels has piqued with the advent of fossil fuel depletion and stringent emissions regulations [1]. Various authors have investigated the effect of bio-fuels, including biodiesel, on diesel engine performance and emissions [2]. Both experimental and theoretical studies with biodiesel indicate a significant decrease in particulate and soot emissions; however, an increase in the formation of nitric oxide (NO) relative to petroleum diesel has been observed with biodiesel [3]. This observed increase in NO emissions for biodiesel has curtailed use of neat biodiesel in diesel engines. This provides motivation to improve our current understanding of factors that influence fundamental mechanisms, which drive an increase in NO emissions for biodiesel relative to petroleum diesel, to reduce NO emissions in engines using biodiesel.

1.2 Background

The three fundamental mechanisms, which govern NO formation in a diesel engine, are thermal, prompt and fuel-bound nitrogen. The thermal mechanisms are a set of temperature dependent reactions that involve NO formation from atmospheric nitrogen in combustion of near-stoichiometric fuel-air mixtures. Reactions (1) - (3) represent the corresponding thermal mechanisms [4]:



This thesis follows the style of Combustion and Flame.



The prompt mechanisms are a set of reactions that produce NO when either nitrogen in the fuel-air mixture reacts with hydrocarbon radicals or HCN forms from fuel-bound nitrogen. The fuel-bound nitrogen mechanisms, which are sensitive to the air-fuel ratio of a mixture, involve NO formation from combustion of oxygen and nitrogen bound to the fuel molecule in the fuel-air mixture.

Various authors have discussed the factors that may influence the relative contributions of the described NO formation mechanisms and drive an increase in NO emissions for biodiesel in the biodiesel literature. A comparative literature review [5] on relative contributions of NO emissions and observed differences in NO emissions between biodiesel and petroleum diesel identifies fuel-bound oxygen, fuel-bound nitrogen, and post-flame gas temperature as potential contributors to observed increases in thermal NO emissions for biodiesel. The authors for this study note that increases in adiabatic flame temperature and ignition delay, a decrease in radiation heat transfer, and advances in injection timing because of fuel's physical and chemical properties strongly influence the post-flame gas temperature for biodiesel and result in increased NO emissions for biodiesel. The effect of fuel-bound oxygen in biodiesel on NO emissions however is disputed in the literature [6].

Compared to petroleum diesel ($\text{C}_{14.09}\text{H}_{24.78}$), biodiesel ($\text{C}_{18.74}\text{H}_{34.43}\text{O}_2$) contains 10-12 wt% oxygen [7]. Theoretically, the presence of additional oxygen in the fuel-air mixture improves combustion efficiency and results in decreased particulate and soot

emissions. NO emissions are expected to increase with an increase in oxygen availability in the fuel-air mixture. Several experimental studies [8-12] support the theorized increase in NO emissions when additional oxygen is supplied with the intake air to the fuel-air mixture. Conversely, Lapuerta *et al.* cite several studies [13-15] that dismiss the role of fuel-bound oxygen in biodiesel on increases in NO emissions. Close reviews of [13-15], however, suggest that the inferences drawn on the effect of fuel-bound oxygen on NO emissions in [6] are questionable and can benefit from further investigation. Therefore, the current study investigates the effect of fuel-bound oxygen content in biodiesel on increases in NO emissions with biodiesel relative to petroleum diesel under an equivalent oxygen environment.

1.3 Objective

The research objective of the current study is to computationally determine if biodiesel and petroleum diesel yield equivalent NO concentrations with the same oxygen equivalence ratio in a 0-D homogeneous reactor, to explain the role of fuel-bound oxygen in biodiesel on NO emissions increases with biodiesel. While several researchers [3, 16-19] have compared the effects of oxygenated and non-oxygenated fuels under equivalent oxygen environments on diesel combustion and emissions to evaluate the emissions reduction effectiveness of both techniques, only three studies [16, 17, 19] provide some original insight on differences in NO emissions for oxygenated fuels relative to non-oxygenated fuels under a comparable oxygen environment. These studies however do not use the oxygen equivalence ratio (described later) as measure of comparison between the oxygenated and non-oxygenated fuels. Only study [17] isolates

the effect of fuel-bound oxygen addition on oxides of nitrogen ($\text{NO}_x = \text{NO} + \text{NO}_2$) emissions, however, for ether-blends. Biodiesel is a long chain mono alkyl methyl or ethyl ester of fatty acids, derived from vegetable oils and animal fats. Moreover, authors of studies [3, 16, 17, 19] have not compared the dominant NO formation (or destruction) mechanisms for either biodiesel or petroleum diesel, to explain the role of fuel-bound oxygen in biodiesel on increases in NO emissions with biodiesel. The findings from the literature [16, 17, 19], which serve as motivation for the current objective, are described below:

1. Zannis *et al.* [16] evaluated the effects of oxygenated and non-oxygenated fuels on NO emissions under comparable oxygen mole fractions in the fuel-air mixture using a two-dimensional multi-zone combustion model and found that the oxygenated fuels yield higher NO emissions relative to the non-oxygenated fuel with comparable oxygen mole fractions in the fuel-air mixture. They conducted their study at constant engine torque, 2500 revolutions per minute (rpm) and 80% load condition for the cases presented in Table 1. The 0 wt% fuel oxygen content and 21% v/v intake air oxygen corresponds to 20.9% v/v for the oxygenated fuel case in Table 1 and to the 21% v/v oxygen for the non-oxygenated fuel; the 9 wt% and 21.2% v/v to 21.1% v/v oxygen for the oxygenated fuel and to the 21.2% v/v oxygen for the non-oxygenated fuel; and so forth. The authors noted an early initiation of NO formation (because of higher gas temperatures in the early phase of combustion) and an increase in peak NO concentrations with an increase in oxygen content of the oxygenated fuel blends and the non-oxygenated

base fuel relative to base fuel with 21% v/v oxygen in the intake air. The higher yield in NO concentrations at equivalent oxygen mole fractions for the oxygenated fuels is attributed to easy availability of fuel-bound oxygen for combustion.

Table 1.

Comparison cases for oxygenated and non-oxygenated fuels under comparable oxygen environments. DI1: base fuel, modeled as $C_{12}H_{24}$, for both the oxygenated and the non-oxygenated fuels; GLY30, DGM50, DGM75: a blend of base fuel and ethers ($C_6H_{14}O_3$, and $C_{12}H_{26}O_3$) at blending ratio of 30%, 50%, and 75% by mass; DGM: neat diglyme. Table reproduced, and modified in part, from [16].

Fuel	Oxygenated Fuel-Air Mixture			Non-Oxygenated Fuel-Air Mixture
	Fuel Oxygen Content (wt. %)	Intake-Air Oxygen (% v/v)	Oxygen in Fuel-Air Mixture (% v/v)	Oxygen in the Fuel-Air Mixture (% v/v)
DI1	0	21	20.9	21
GLY30	9	21.2	21.1	21.2
DGM50	15.9	21.5	21.4	21.5
DGM75	25.3	21.9	21.8	21.9
DGM	35.8	22.6	22.5	22.6

Moreover, Zannis *et al.* found a non-linear correlation between the NO emissions (in parts per million) in the exhaust and oxygen in the fuel-air mixture (% v/v) for the oxygenated fuels, and a linear correlation between the NO emissions in the exhaust and oxygen in the fuel-air mixture for the non-oxygenated fuel. They also observed that the oxygenated fuel produced twice as much NO as the non-oxygenated fuel when the oxygen in the fuel-air mixture was maximized to 22.5 % v/v for the oxygenated fuel and 22.6 % v/v for the non-oxygenated fuel. The noted differences in the trends between the oxygenated

and the non-oxygenated fuels are attributed to fuel-bound oxygen content, physical properties, and molecular structure of the ether-blended fuels. No attempt is made to isolate the effects of fuel-bound oxygen addition on NO_x emissions in their study.

2. Song *et al.* [17] conducted an experimental study to compare the relative effects of oxygenated and non-oxygenated fuels on diesel combustion and NO_x emissions under comparable oxygen-to-carbon (O/C) ratios. The authors ran their 1.9 L TDI turbocharged diesel engine at 1900 rpm and 75% load condition for base diesel ($\text{C}_{15}\text{H}_{27.66}$) at O/C of 4.6, and for glycol ethers ($\text{C}_4\text{H}_{10}\text{O}_2$ and $\text{C}_6\text{H}_{14}\text{O}_3$) blends and 1, 3- dioxolane ($\text{C}_3\text{H}_6\text{O}_2$) blend at O/C of 4.8 and 5.1. Glycol ethers are linear structure molecules. 1, 3-dioxolane is a ring-structured molecule. Conversely (to [16]), they found that the non-oxygenated fuel produces higher NO_x emissions compared to the oxygenated fuels at the same O/C ratio. The NO_x emissions for comparable O/C ratio in their study increase (in order) for the 1, 3-dioxolane, the glycol ethers, and the oxygenated intake-air and base diesel mixture. The high NO_x yield for the oxygenated intake-air and base diesel mixture is attributed to either increased availability of oxygen in the fuel-air mixture or high combustion temperatures in a lean environment, which in the authors' opinion augment thermal NO_x formation kinetics. The differences in NO_x emissions between the two oxygenated fuels for the same O/C ratio are attributed to differences in molecular structure of fuels. Song *et al.* also isolated the chemical effect of fuel-bound oxygen on NO_x emissions for both the glycol

ethers blends and the 1, 3-dioxolane blends relative to alkane blends for both fuel-blends and found that NO_x emissions do not vary significantly with oxygen addition for both fuel-blends.

3. Donahue *et al.* [19] compared the effects of oxygenated and non-oxygenated fuels on NO_x emissions relative to base diesel experimentally at comparable injection timings. Their experimental study was conducted at 1200rpm and 75% load condition for base diesel ($\text{C}_{15}\text{H}_{27.66}$), methyl t-butyl ether (MTBE, $\text{C}_5\text{H}_{12}\text{O}$) blend, and 22 and 23 vol. % oxygen in the intake air for the base diesel. The authors found that the oxygenated intake-air and base diesel mixtures result in higher NO_x emissions compared to the oxygenated fuels, where the magnitude of increase in NO_x emissions depends on the fuel injection timing. The MTBE blend has little effect on NO_x emissions relative to base diesel.

The authors also made an analytical comparison using O/C ratio for the base diesel, the MTBE blend, and the 23 vol. % oxygen content in the intake-air and base diesel mixture to explain differences in local fuel plume environment and global in-cylinder oxygen concentrations for the fuels. They found that the MTBE blend adds about 4.6% oxygen, and the 23 vol. % oxygen adds about 9.5% oxygen relative to base diesel to the local fuel plume environment. The MTBE blend yields insignificant change in global oxygen concentration. The 23 vol. % oxygen increases the global oxygen concentration by about 9.5% relative to base diesel. Based on these findings, Donahue *et al.* conclude that increased

formation of NO_x emissions for the non-oxygenated fuel and oxygen added intake-air mixture (as opposed to the oxygenated fuels) result solely from increased local and global presence of oxygen, regardless of the method of oxygen addition.

To summarize, there is no consensus in the literature on the effect of oxygenated and non-oxygenated fuels on NO_x emissions under equivalent oxygenation, and only Song *et al.* have isolated the effect of fuel-bound oxygen addition on NO_x emissions. While Zannis *et al.* found high NO yields for the oxygenated fuels at comparable oxygen mole fractions, Song *et al.* observed high NO yields for the non-oxygenated fuel at comparable oxygen-to-carbon ratios for the ether-blends (relative to petroleum diesel). Zannis *et al.* attribute the high NO yield for oxygenated fuels to high in-cylinder temperature and easy availability of fuel-bound oxygen for combustion. Conversely, Song *et al.* attribute the small NO yield for oxygenated fuels to low in-cylinder temperature and low availability of fuel-bound oxygen for combustion. Donahue *et al.* did not conduct their study at comparable oxygen percentage in the fuel-air mixture; however, they conjecture similar NO_x emissions between oxygenated and non-oxygenated fuels at comparable oxygenation. This is because they attribute low emissions only to increases in the local oxygen content in the fuel plume and the in-cylinder mixture. Song *et al.*, who isolated the effect of fuel-bound oxygen addition on NO_x emissions, found an insignificant increase in NO_x emissions through fuel-bound oxygen addition using ether-blends.

Identified studies [16, 17] do not use a comparable measure for quantifying the amount of oxygen in the fuel-air mixture. While Zannis *et al.* [16] use comparable oxygen mole fraction to evaluate differences in NO_x emissions between oxygenated and non-oxygenated fuels at various oxygenation levels, Song *et al.* [17] use comparable oxygen-to-carbon ratio in their study. It may therefore be inappropriate to compare and assess the validity of their results against each other to answer our objective. Studies that characterize the effect of equivalent oxygenation between oxygenated and non-oxygenated fuels on NO_x emissions using the oxygen ratio, a more appropriate measure of oxygen percentage in the fuel-air mixture, do not exist in the literature. The oxygen ratio is the “amount of oxygen available in reactants divided by amount required for stoichiometric combustion, neglecting oxygen bound in stable species” [18]. It is a more accurate measure of in-cylinder stoichiometry than the oxygen mass fraction, the oxygen-to-carbon ratio, and the equivalence ratio because the oxygen ratio guarantees that two or more mixtures contain equal percentage of oxygen needed for stoichiometric combustion [18].

None of the summarized studies compare the effects of equivalent oxygenation on NO_x emissions between biodiesel (an ester-blend) and petroleum diesel. The trends for NO_x emissions are expected to differ either qualitatively or quantitatively between esters and ethers based on previous work of Mueller *et al.* [18]. The authors of [18] examined the soot reduction tendency of di-butyl maleate (DBM, a biodiesel like oxygenate) and tri-propylene glycol methyl ether (TPGME) in their study and found that DBM is less effective than TPGME in reducing in-cylinder soot, regardless of oxygen-

ratio and charge gas conditions. Their chemical-kinetics simulations show that over 30% of the fuel-bound oxygen in DBM is unavailable for soot precursor reduction because DBM uses the available oxygen in production of CO₂ before formation of soot precursors. Given these results and current knowledge about the intimate link between a fuel's soot reduction chemistry and NO production chemistry, a different effect (from the previous studies using ether-blended fuels) is expected for NO emissions under equivalent oxygenation between biodiesel and petroleum diesel.

Consequently, the effects of equivalent oxygenation on NO_x emissions with the same oxygen equivalence ratio are investigated for biodiesel and petroleum diesel using commercially available software, to explain the role of fuel-bound oxygen in biodiesel on NO_x emissions increases with biodiesel relative to petroleum diesel. A fundamental chemical kinetics simulation, decoupled from application, is conducted because it is difficult to experimentally resolve the effect of fuel-bound oxygen in biodiesel on NO_x emissions in a complex environment, such as the internal combustion engine. Since chemical kinetics determines concentrations of NO_x emissions in the exhaust, a chemical kinetics modeling approach is employed. This approach also aids in identifying key differences in NO_x formation mechanisms between biodiesel and petroleum diesel. Knowing the fundamental differences in NO_x formation mechanisms for both fuels may lead to an improved understanding of how fuel-bound oxygen influences NO_x formation for biodiesel relative to petroleum diesel.

2. NUMERICAL MODELING

Numerical simulations are run for petroleum diesel and biodiesel with the same oxygen equivalence ratio in a constant pressure zero-dimensional (0-D) homogeneous reactor in CHEMKIN PRO under adiabatic conditions, to examine the effect of fuel-bound oxygen in biodiesel on NO_x emissions increases with biodiesel relative to petroleum diesel. The basic assumptions embedded in and the mass and species conservation and first law analyses for the 0-D homogeneous model are described in section 2.1. The surrogate fuels and the chemical kinetics mechanisms, needed to run the simulations, are obtained from the literature and discussed in section 2.2. The initial reactor conditions, the initial mole fractions of surrogate fuel-air mixtures, and the model verification process are described in section 2.3. Section 2.4 provides a list of computed data collected to arrive at the conclusions for our study.

2.1 Zero-Dimensional (0-D) Homogenous Reactor

The zero-dimensional (0-D) homogeneous reactor models a closed thermodynamic system, which operates on the following basic assumptions [20]:

1. Spatially averaged or bulk properties can describe the mixture well because mixture is sufficiently mixed.
2. Mixing is fast and mass transport to reactor walls is infinitely fast.
3. Kinetics rates, and not mixing, govern the rate of conversion of reactants to products.

4. Nominal residence time characterizes flow through the reactor.

The mass and species conservation and first law analyses for the 0-D homogeneous reactor are as follows:

Global Mass Conservation for the Closed System:

For a closed system, with no mass addition or subtraction from the reactor surface, the time rate of change of mass is $\frac{d(\rho V)}{dt} = 0$ where ρ is the mixture mass density and V is the reactor volume.

Mass Conservation for Gas Phase Species for the Closed System:

For a closed system, the time rate of change of species is $\sum_{k=1}^{K_g} \rho_k V \frac{dY_k}{dt} = 0$ where ρ_k is the species mass density of the k^{th} species, V is the reactor volume, Y_k is the mass fraction of the k^{th} species, and K_g is the total number of species in the gas phase.

Gas Energy Equation for the Closed System:

For a constant pressure closed system under adiabatic conditions, the time rate of change of internal energy for the control volume is $\frac{dU_{gas}}{dt} = 0$. It should be noted that the control volume consists of the gas mixture alone, and any contribution from the surface phases, the deposited or etched solid phases and the walls to the internal energy is neglected. Under these conditions, the time rate of change of internal energy for the gas mixture is:

$$\frac{dU_{gas}}{dt} = \frac{d(H_{gas} - PV)}{dt} = \frac{dH_{gas}}{dt} = 0 \text{ for a constant pressure, closed system}$$

$$\frac{dH_{gas}}{dt} = \frac{d(\rho V h_{gas})}{dt} = 0, \text{ and } h_{gas} = \sum_{k=1}^{K_g} Y_k h_k; h_k \text{ is the specific enthalpy of pure species}$$

$$\frac{d(\rho V \sum_{k=1}^{K_g} Y_k h_k)}{dt} = \rho V \sum_{k=1}^{K_g} Y_k \frac{dh_k}{dt} + \rho V \sum_{k=1}^{K_g} h_k \frac{dY_k}{dt} + \sum_{k=1}^{K_g} Y_k h_k \frac{d(\rho V)}{dt} = 0; \quad \frac{d(\rho V)}{dt} = 0 \quad \text{from}$$

mass conservation, $\frac{dY_k}{dt} = 0$ from species conservation and $\frac{dh_k}{dt} = c_{pk} \frac{dT_k}{dt}$ where c_{pk} is

the specific heat of the k^{th} species in the gas mixture.

After simplification, the gas energy equation for the 0-D closed system is:

$$\rho V \sum_{k=1}^{K_g} Y_k c_{pk} \frac{dT_k}{dt} = 0 \quad (4)$$

CHEMKIN PRO uses this equation (4) to find temperatures at the prescribed initial conditions in the 0-D homogeneous reactor for the current study.

This 0-D homogeneous reactor does not model a typical diesel engine environment globally because diesel engine combustion is inherently heterogeneous; however, this reactor is sufficient to model combustion phenomena, where locally homogeneous fuel-air mixture pockets exist within the diesel engine. This reactor model is also simple and computationally inexpensive. Hence the 0-D homogeneous reactor is an adequate model to conduct a fundamental analysis in idealized diesel engine

conditions, to examine the role of fuel-bound oxygen in biodiesel on increases in NO_x emissions with biodiesel relative to petroleum diesel.

2.2 Fuel and NO_x Chemistry

N-heptane ($\text{n-C}_7\text{H}_{16}$) and a blend of n-heptane, methyl esters methyl-decanoate ($\text{C}_{11}\text{H}_{22}\text{O}_2$) and methyl 9 decenoate ($\text{C}_{13}\text{H}_{24}\text{O}_2$) are selected as surrogates [21] to model petroleum diesel and biodiesel respectively in CHEMKIN PRO. The reaction species and the detailed chemical kinetics mechanisms for the surrogate fuels are obtained from the literature [21, 22] in CHEMKIN format. The detailed n-heptane mechanism has been validated experimentally in [22] for initial pressures ranging from 3 to 50 atmospheres (atm), initial temperatures from 650 to 1200 Kelvin (K), and equivalence ratios from 0.3 to 1.0 in shock tubes and rapid compression machines. The detailed biodiesel surrogate mechanism has been validated experimentally in [21] for initial temperatures from 800 to 1400 K at 10 atm and an equivalence ratio of 0.5 in a jet-stirred reactor of rapeseed oil methyl esters, and for initial temperatures from 550 to 1100 K at 1 atm and an equivalence ratio of 1.0 in a jet stirred reactor of a mixture of methyl palmitate and n-decane. The jet-stirred reactor is a 0-D homogeneous reactor. The complete NO_x formation chemistry, obtained from the GRI Mechanism 3.0 [23], is integrated into both the n-heptane and biodiesel surrogate blend chemistry. The thermodynamics data for the n-heptane and the biodiesel surrogate blend species is obtained from [22, 21] and extended to include thermodynamics data from [24] for species which participate in NO_x formation. The modified reaction mechanisms and thermodynamics data were uploaded in CHEMKIN PRO for analysis.

2.3 Initial Conditions and Model Verification

2.3.1 Initial Conditions for the 0-D Homogeneous Reactor

The initial temperature and pressure for the 0-D homogeneous reactor are set to 886 K and 60 bars respectively for both n-heptane and the biodiesel surrogate. The selected initial conditions are typical of a diesel engine environment at the start of fuel injection under ordinary operating conditions (eg., 1400 rpm, 50 ft-lb torque). It is recognized that the optimal injection timing and therefore the start of combustion conditions for biodiesel may be different from those of petroleum diesel; however, the same initial conditions are set for the biodiesel surrogate to create a consistent environment between the two fuels. The reactor residence time is set to 3.571 milliseconds (ms). This residence time is typical of the duration of combustion in a diesel engine, running at 1400 rpm and 50 ft-lbs torque. The heat loss from the 0-D homogeneous reactor is set to zero (i.e. adiabatic conditions). The equivalence ratio and initial mole fractions of the fuel-air mixture are calculated, as shown in sub-sections 2.3.1.1 and 2.3.1.2 respectively, for both n-heptane and the biodiesel surrogate and are input into CHEMKIN PRO.

2.3.1.1 Equivalence Ratio Calculation

The equivalence ratio for the n-heptane is set to 1.0. This is because we assumed complete combustion of n-heptane under our initial conditions. This is a fair assumption because diffusion combustion happens under stoichiometric or near-stoichiometric conditions in a diesel engine. The oxygen equivalence ratio is then used to characterize fuel-mixture stoichiometry in the reactor for both the n-heptane and the biodiesel

surrogate. The oxygen equivalence ratio (ϕ_Ω) is “an instantaneous measure of the proximity of a reactant mixture to its stoichiometric condition” [25]. It is an appropriate measure to quantify the mixture stoichiometry when the fuel molecules contain oxidizer elements (such as O) or when the oxidizer elements contain fuel elements (such as C or H). The oxygen equivalence ratio is defined in [25] as equation (5), where the fuel oxygen ratio (Ω_f) and the oxidizer oxygen ratio (Ω_{ox}) are defined in equations (6) and (7) respectively:

$$\phi_\Omega \equiv \frac{1}{\Omega} = \frac{\phi + \frac{(1 - \phi - \Omega_f)}{\Omega_{ox}}}{1 - \Omega_f \left(1 - \phi + \frac{\phi}{\Omega_{ox}} \right)} \quad (5)$$

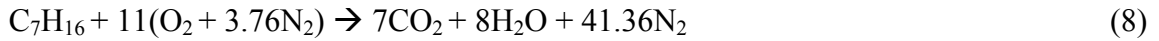
$$\Omega_f \equiv \frac{\sum_i a_i n_{o,i}}{\sum_i a_i \left(2n_{C,i} + \frac{1}{2}n_{H,i} \right)} \quad (6)$$

$$\Omega_{ox} \equiv \frac{\sum_j b_j n_{o,j}}{\sum_j b_j \left(2n_{C,j} + \frac{1}{2}n_{H,j} \right)} \quad (7)$$

where a_i are the number of moles of the i^{th} species in the reactants and $n_{O,i}$, $n_{C,i}$, and $n_{H,i}$ are the number of atoms of oxygen, carbon, and hydrogen, respectively, in the i^{th} species in the reactants in equation (6), and b_j are the number of moles of the j^{th} species in the

oxidizers and $n_{O,j}$, $n_{C,j}$, and $n_{H,j}$ are the number of atoms of oxygen, carbon, and hydrogen, respectively, in the j^{th} species in the oxidizers in equation (7).

An oxygen equivalence ratio of 1.0 is determined for the n-heptane based on Mueller's definition. This is because the stoichiometric reaction for n-heptane lends itself to $\Omega_{f, \text{n-heptane}}$ of zero (because the fuel does not contain oxygen atoms) and $\Omega_{\text{ox, oxygen}}$ of ∞ (because the oxidizer does not contain hydrogen or carbon atoms). The nitrogen species are neglected in the oxygen equivalence calculation because nitrogen is neither a fuel nor an oxidizer. The stoichiometric reaction for the n-heptane is shown in equation (8):



Since CHEMKIN PRO requires the user to input the equivalence ratio to define fuel-air mixture stoichiometry, the equivalence ratio for the biodiesel surrogate is calculated at the same oxygen equivalence ratio as the n-heptane. This calculation is shown in (9). Equation (8) shows that an oxygen equivalence ratio of 1.0 for n-heptane results in an equivalence ratio of 1.0 for the biodiesel surrogate.

$$\begin{aligned} \phi_{\Omega, \text{biodiesel}} &= \phi_{\Omega, \text{n-heptane}} = \frac{\phi_{\text{biodiesel}}}{1 - \Omega_{f, \text{biodiesel}} (1 - \phi_{\text{biodiesel}})} = 1, \Omega_{\text{ox}} = \infty \\ \phi_{\text{biodiesel}} (1 - \Omega_{f, \text{biodiesel}}) &= (1 - \Omega_{f, \text{biodiesel}}) \\ \phi_{\text{biodiesel}} &= 1 \end{aligned} \quad (9)$$

As a result, an equivalence ratio of 1.0 is set for both the n-heptane and the biodiesel surrogate in CHEMKIN PRO.

2.3.1.2 Initial Mole Fractions Calculation

The initial mole fractions of the n-heptane and the biodiesel surrogate blend, and oxygen and nitrogen in the fuel-air mixture are calculated for the stoichiometric reactions from equations (10) and (11) respectively. These initial mole fractions are determined to be 1.0 for the n-heptane, 0.3333 each for the biodiesel surrogate blend components, 0.2100 for the oxygen and 0.7899 for the nitrogen in the stoichiometric reactions.

$$\text{Fraction}_{i, \text{fuel}} = \frac{n_{i, \text{fuel}}}{n_{\text{total}, \text{fuel}}} \quad (10)$$

$$\text{Fraction}_{i, \text{oxidizer}} = \frac{n_{i, \text{oxidizer}}}{n_{\text{total}, \text{oxidizer}}} \quad (11)$$

The stoichiometric reaction for the n-heptane-air mixture is shown earlier in (8). The stoichiometric reaction for the biodiesel surrogate-air mixture is shown in (12).



The computed initial mole fractions of the fuel-air mixture components are input to CHEMKIN PRO for n-heptane and the biodiesel surrogate blend. Table 2 summarizes the initial conditions for the biodiesel and the petroleum diesel in table format.

2.3.2 Model Verification

The constant pressure 0-D homogeneous reactor is verified against the constant pressure equilibrium (EQUIL) reactor in CHEMKIN PRO, and the constant pressure EQUIL reactor is verified against the constant pressure model in Adiabatic Flame Temperature Program (AFTP). The EQUIL reactor computes the equilibrium

composition of an ideal gas-phase mixture via minimization of the Gibb's Free Energy. The AFTP is an independent program, which operates on the same principles as the EQUIL reactor. The 0-D homogenous reactor is verified against the EQUIL reactor for both the n-heptane and the biodiesel surrogate. The EQUIL reactor however is verified against the AFTP for the n-heptane only. This is because the biodiesel surrogate is not available for modeling in the AFTP.

Table 2.
Initial conditions for Biodiesel and Petroleum Diesel.

	Biodiesel	Petroleum Diesel
Fuel Model	n-Heptane + Methyl Esters	n-Heptane
Molecular Formula	$nC_7H_{16} + C_{13}H_{24}O_2 + C_{11}H_{22}O_2$	nC_7H_{16}
Equivalence Ratio	1	1
Mole Fraction, Fuel	0.3333 per component	1
Mole Fraction, Air	$O_2 : 0.21; N_2 : 0.7899$	$O_2 : 0.21; N_2 : 0.7899$
Initial Temperature	886 K	886 K
Initial Pressure	60 bars	60 bars
Residence Time	3.571 ms	3.571 ms
Heat Loss	0	0

The 0-D homogeneous reactor is compared with the EQUIL reactor and the EQUIL reactor with the AFTP model under the same initial temperature (886 K) and pressure (60 bars) in adiabatic conditions with equivalence ratios ranging from 0.2 to 2.0. The residence time for the homogeneous reactor is incremented to find if the species in the homogeneous reactor would reach equilibrium given sufficient time in the reactor. The reaction species in the homogeneous reactor are determined to have reached

equilibrium when the adiabatic flame temperature and species concentrations at all equivalence ratios matched those of the EQUIL reactor for the n-heptane and the biodiesel surrogate. The adiabatic flame temperature and species concentrations at all equivalence ratios for the EQUIL reactor are matched with the AFTP model for the n-heptane to verify the adiabatic flame temperature and species concentrations from the EQUIL reactor.

The adiabatic flame temperature and species concentrations trends of the biodiesel surrogate at five initial conditions selected from the experimental ranges specified in [21] are also compared to the initial conditions of our study in the homogeneous reactor. This comparison is made to find a qualitative validation for the biodiesel surrogate under our initial conditions because the fuel chemistry for the biodiesel surrogate has only been validated experimentally for conditions different from the current study.

2.4 Data Collection

The adiabatic flame temperature and species concentrations for NO, NO₂ and O₂ for the n-heptane and the biodiesel surrogate are computed under the initial conditions described in sections 2.3.1 and 2.3.2 as a function of the equivalence ratio and the reactor residence time. The rate of molar fuel conversion is also collected for the biodiesel surrogate and the n-heptane. The rates of production (or destruction) of NO species are also collected for nominal NO concentrations of 2000, 4000, and 6000 ppmvd and at reactor residence time of 3.571 ms for both the n-heptane and the biodiesel surrogate.

3. RESULTS AND DISCUSSION

3.1 Model Verification

The 0-D constant pressure homogeneous reactor adequately models the combustion temperatures and the concentrations of oxides of nitrogen and oxygen for the n-heptane. As seen from Fig. 1, the temperatures and the concentrations of NO_x and O_2 in the homogeneous reactor reasonably match those from the EQUIL reactor when the species residence time in the reactor is incremented to 20 seconds for the initial conditions for the n-heptane. This is especially true for the oxygen equivalence ratio of 1.0 (point of interest in this study) and for the fuel-rich conditions. Any discrepancies between computed values for temperatures and concentrations of NO_x and O_2 in the fuel-lean conditions are likely from non-convergence of the solution. It should be noted that the temperatures and concentrations of NO_x and O_2 from the homogeneous reactor match those from the EQUIL reactor even at 3.571 ms for oxygen equivalence ratio ≥ 1.0 ; however, the residence time is incremented to 20 seconds to match the temperatures and concentrations of NO_x and O_2 for the fuel-lean conditions. Moreover, Fig. 2 shows that the temperatures and concentrations of NO_x and O_2 in the EQUIL reactor reasonably match those from the AFTP model for the n-heptane. Since the only difference between the EQUIL reactor and the AFTP model is the number of participating species in the model, the observed differences between computed temperatures and concentrations of NO_x and O_2 are attributed to the number of participating species. The EQUIL model

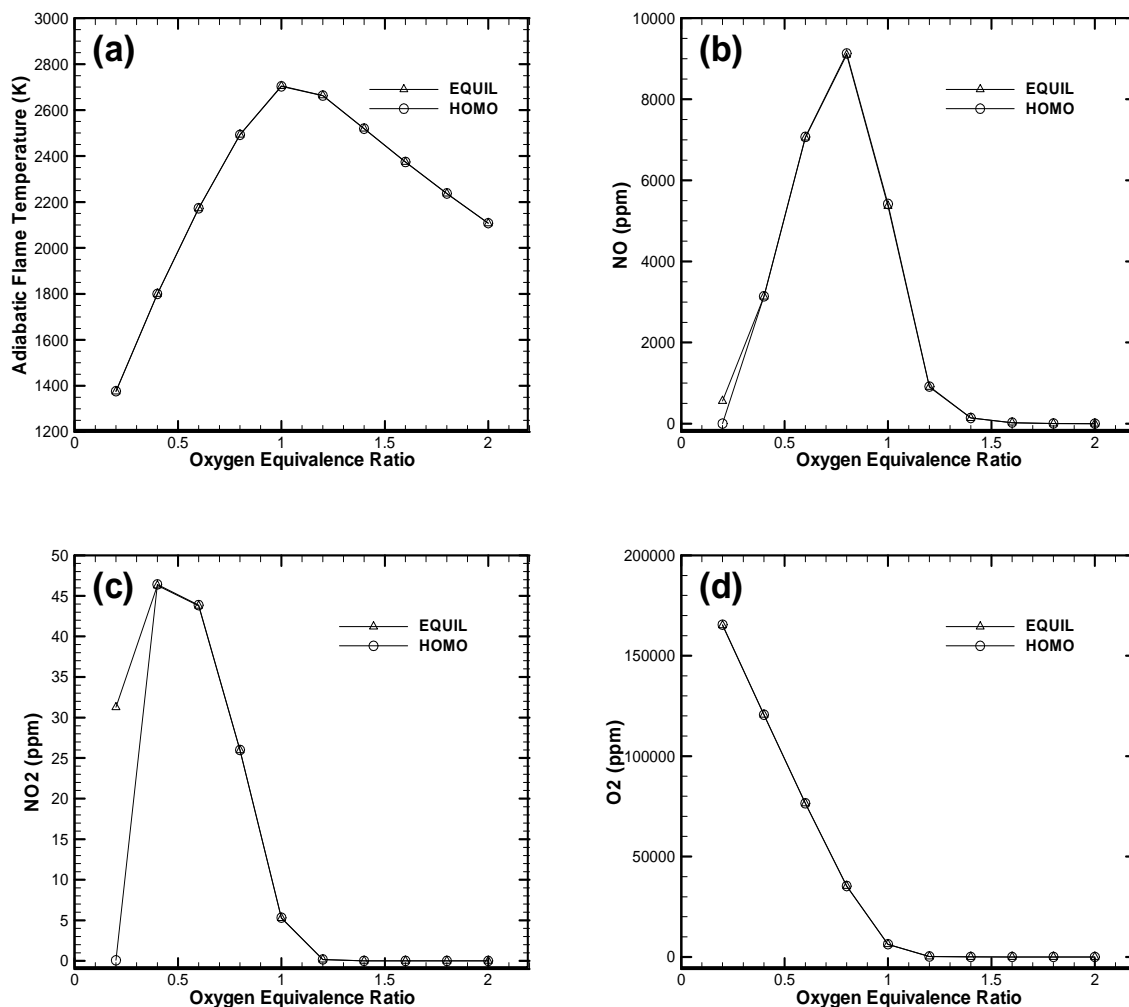


Fig. 1. Comparison between computed values from a homogeneous reactor (HOMO) and equilibrium reactor (EQUIL) in CHEMKIN PRO for (a) temperature (K), (b) NO (ppm), (c) NO₂ (ppm), and (d) O₂ (ppm) as a function of oxygen equivalence ratio for n-heptane in a zero-dimensional constant pressure reactor with initial temperature and pressure at 886 K and 60 bars respectively, at residence reactor time = 20 seconds.

however is more accurate compared to the AFTP model because the EQUIL model has a higher number of species that partake in the computed solution. This gives further

confidence in the predicted temperatures and concentrations of NO_x and O_2 in the 0-D constant pressure homogeneous reactor for the n-heptane.

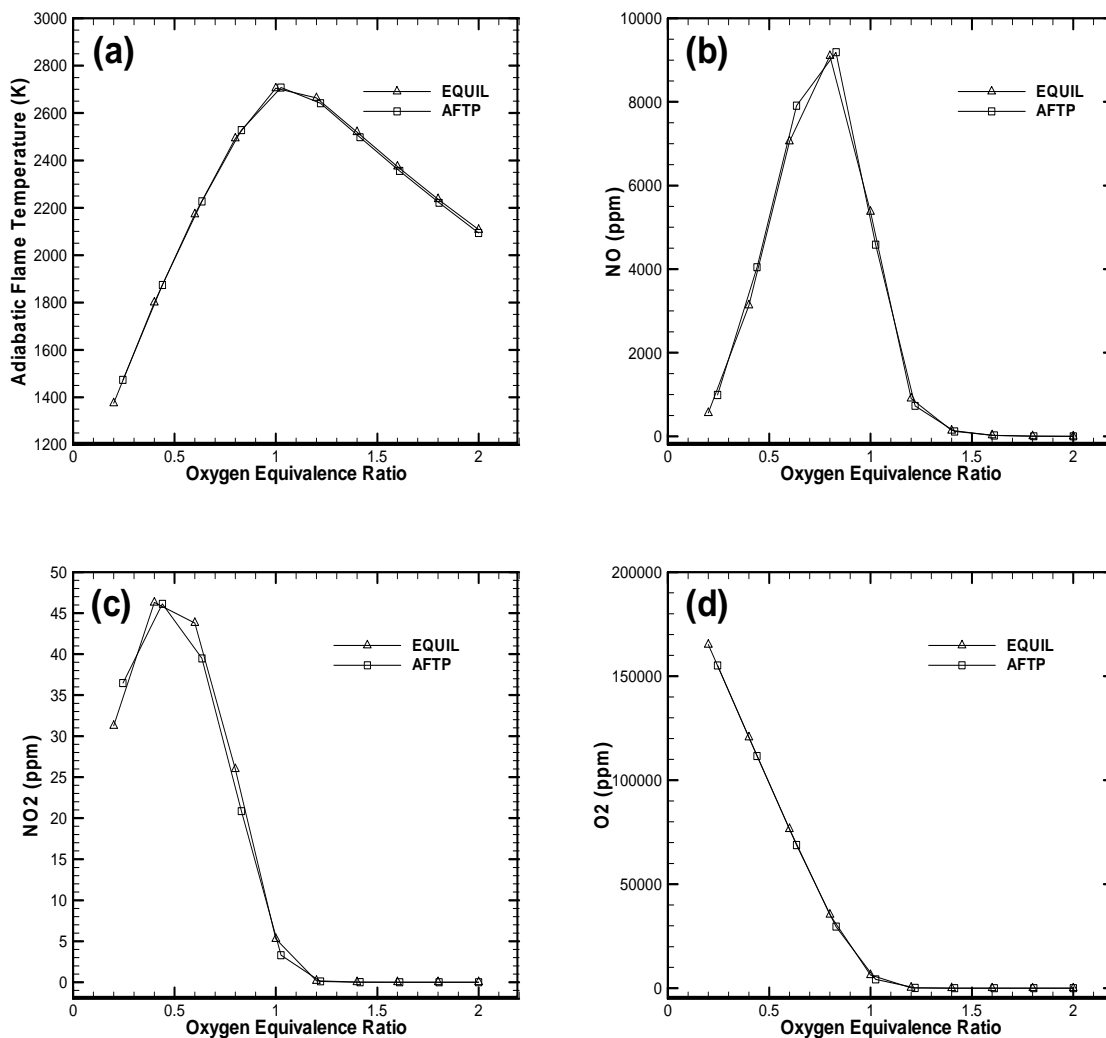


Fig. 2. Comparison between computed values from equilibrium reactor (EQUIL) in CHEMKIN-PRO and Adiabatic Flame Temperature Program (AFTP) for (a) temperature (K), (b) NO (ppm), (c) NO₂ (ppm), and (d) O₂ (ppm) as a function of oxygen equivalence ratio for n-heptane in a zero-dimensional constant pressure reactor with initial temperature and pressure at 886 K and 60 bars respectively.

Similarly, the 0-D constant pressure homogeneous reactor adequately models the combustion temperatures and the concentrations of oxides of nitrogen and oxygen for the biodiesel surrogate. As seen in Fig. 3, the temperatures and concentrations of NO_x and O_2 in the homogeneous reactor approach those from the EQUIL reactor when the species residence time in the reactor is incremented from 0.0006 seconds to 1 second to 3 seconds. The three second run was computed for an oxygen equivalence ratio of 1.0 only because the run is computationally expensive. (The computed temperature and concentrations of NO_x and O_2 for the oxygen equivalence ratio of 1.0 lies on the EQUIL line.) Since the temperatures and concentrations of NO_x and O_2 in the homogeneous reactor approach those from the EQUIL reactor with an increase in species residence time in the reactor, it is reasonable to believe that the homogeneous reactor solution will approach the solution from the EQUIL reactor if sufficient reaction time is given to the biodiesel surrogate species. This trend gives some confidence in the predicted temperatures and concentrations of NO_x and O_2 in the 0-D constant pressure homogeneous reactor for the biodiesel surrogate.

Moreover, the use of biodiesel surrogate from [21] was found to be acceptable under the initial conditions of this study when the temperatures and concentrations of O_2 at the initial conditions of this study were compared to the initial condition ranges experimentally validated in [21]. The trends for computed temperatures and concentrations of O_2 as a function of reactor residence time for five initial conditions selected from the ranges specified in [21] are shown in Fig. 4. As seen in Fig. 4, the computed temperatures and concentrations of O_2 qualitatively mimic the behavior of

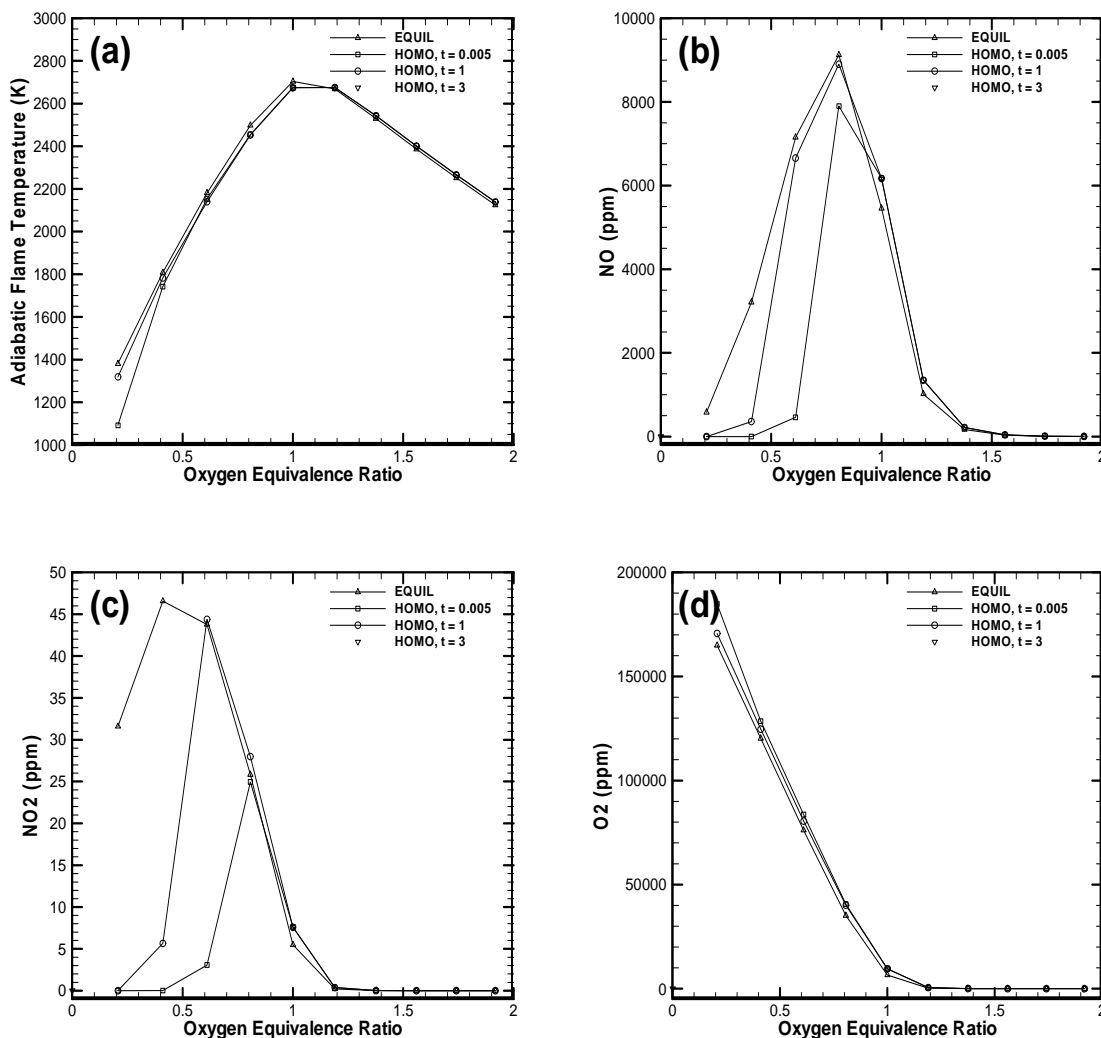


Fig. 3. Comparison between computed values from a homogeneous reactor (HOMO) and equilibrium reactor (EQUIL) in CHEMKIN PRO for (a) temperature (K), (b) NO (ppm), (c) NO₂ (ppm), and (d) O₂ (ppm) as a function of oxygen equivalence ratio for a biodiesel surrogate in a zero-dimensional constant pressure reactor with initial temperature and pressure at 886 K and 60 bars respectively, at residence reactor time = 0.006, 1, and 3 seconds.

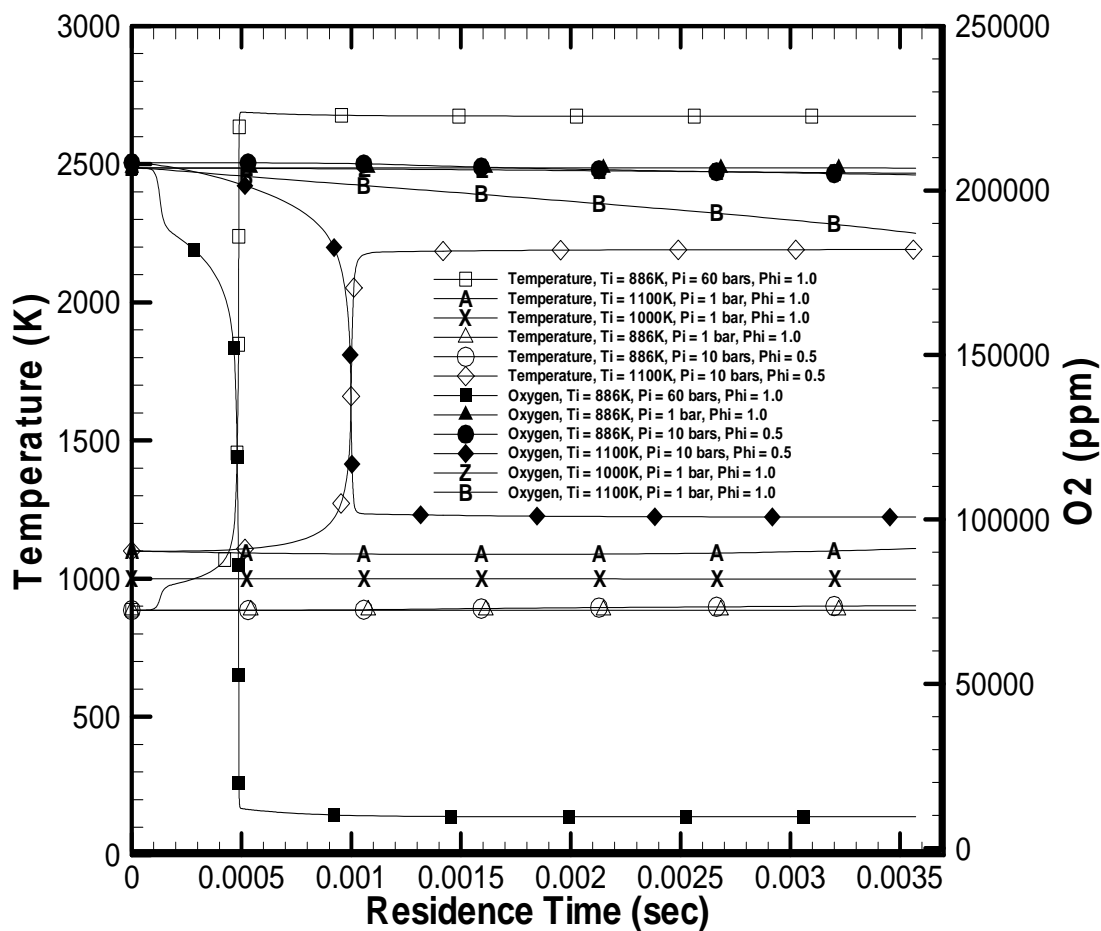


Fig. 4. Comparison of trends for computed temperature and oxygen as a function of reactor residence time in a zero-dimensional constant pressure homogeneous reactor between initial conditions of our study ($T_i = 886$ K, $P_i = 60$ bars, $\phi = 1.0$) and five initial conditions selected from the ranges specified in [21] for which the biodiesel surrogate mechanisms have been experimentally validated in [21].

those from this study when the initial temperature and pressure are increased to 1100 K and 10 bars. This similarity in trends for high temperatures and pressures between the initial conditions of the current study (886K, 60 bars) and [21] (1100K, 10 bars) gives

reason to believe that the biodiesel surrogate would behave similarly if validated experimentally for the initial conditions in the current study. Hence the use of the biodiesel surrogate from [21] for computations of temperatures and concentrations of NO_x and O_2 at the initial conditions in the current study is valid.

3.2 Numerical Modeling

The biodiesel surrogate yields higher NO_x concentrations than the n-heptane at the end of combustion for the same oxygen equivalence ratio because oxygen in the biodiesel surrogate-air mixture is used less efficiently compared to the n-heptane-air mixture. Fig. 5 shows that the NO_x ($\text{NO} + \text{NO}_2$) formation for the biodiesel surrogate began a few microseconds after the NO_x formation for the n-heptane, increased drastically at a rate similar to the n-heptane, and then surpassed the NO_x formation for n-heptane before it leveled to the NO_x value seen at the end of combustion. The same trend is shown for NO and NO_x emissions on a dry basis in Fig. 6. Moreover, as seen in Fig. 5, the contribution of NO_2 to NO_x formation for the biodiesel surrogate is higher than the n-heptane; however, the value is insignificant when making a comparison between the NO_x formation of the biodiesel surrogate and the n-heptane. Hence, the contribution of NO_2 to total NO_x formation can be neglected. In other words, NO is the majority of the NO_x for both the biodiesel surrogate and the n-heptane. Thus, NO formation is analyzed next for the two surrogates.

The thermal NO was found to be a major contributor to formation of NO when the total NO was subdivided into thermal and non-thermal NO formation for both the biodiesel surrogate and the n-heptane. Fig. 7 shows the formation of NO , plotted as

thermal and non-thermal NO contribution to total NO, as a function of reactor residence time. As seen in Fig. 7, the thermal NO to the total NO for the biodiesel surrogate decreased with an increase in residence reactor time before the n-heptane did, and then increased drastically to its peak a few microseconds after the n-heptane at a rate similar to the n-heptane. Later, the thermal NO to total NO for the biodiesel surrogate decreased and leveled to a thermal NO value higher than the n-heptane. Conversely, the non-ther-

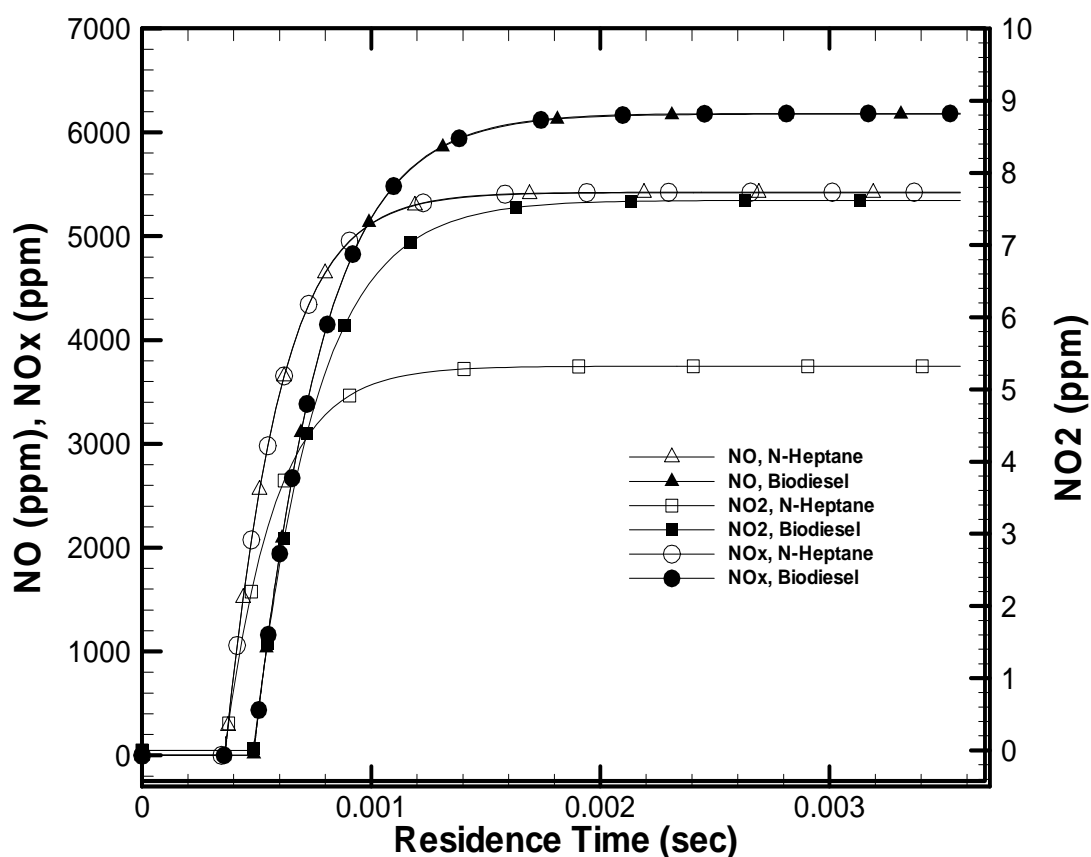


Fig. 5. Computed NO, NO₂ and NO_x as a function of reactor residence time in a zero-dimensional constant pressure homogeneous reactor at initial temperature and pressure of 886 K and 60 bars respectively for n-heptane and the biodiesel surrogate.

-mal NO to the total NO for the biodiesel surrogate increased with an increase in residence reactor time before the n-heptane did, and then decreased drastically to its valley a few microseconds after the n-heptane at a rate similar to the n-heptane. Later, the non-thermal NO to total NO for the biodiesel surrogate increased and leveled to a non-thermal NO value lower than the n-heptane. The dominance of the thermal NO formation during combustion for both the surrogates is thus evident from Fig. 7.

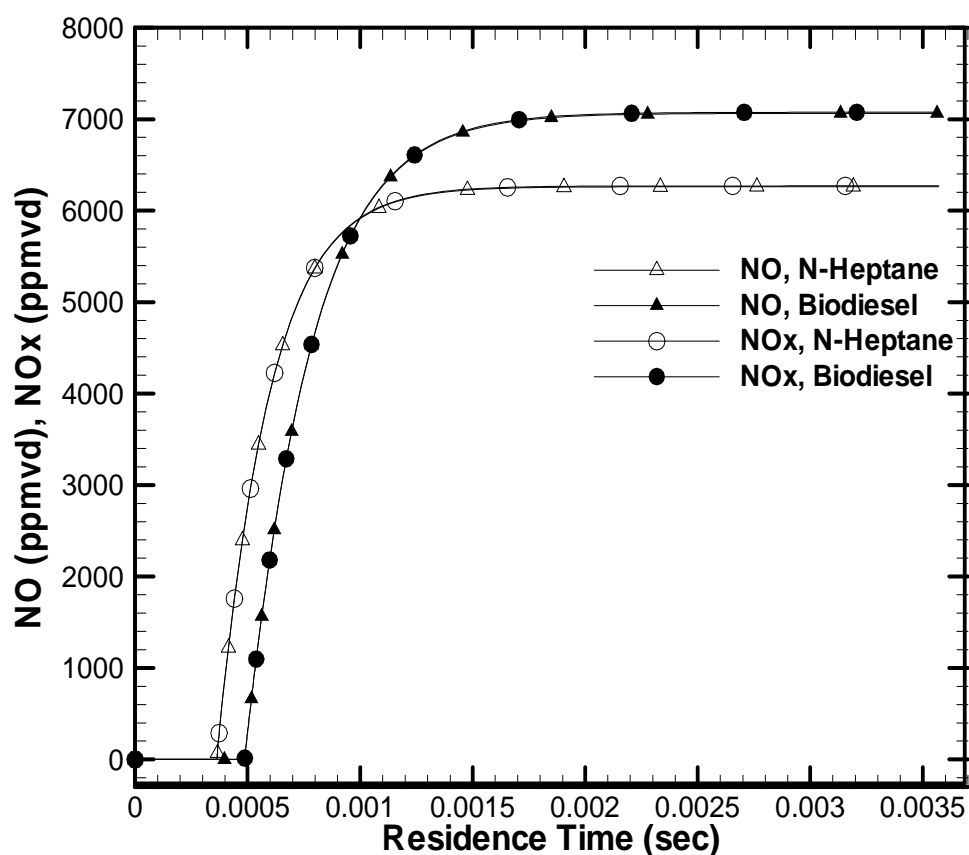


Fig. 6. Computed NO and NO_x on a dry basis as a function of reactor residence time in a zero-dimensional constant pressure homogeneous reactor at initial temperature and pressure of 886 K and 60 bars respectively for n-heptane and the biodiesel surrogate.

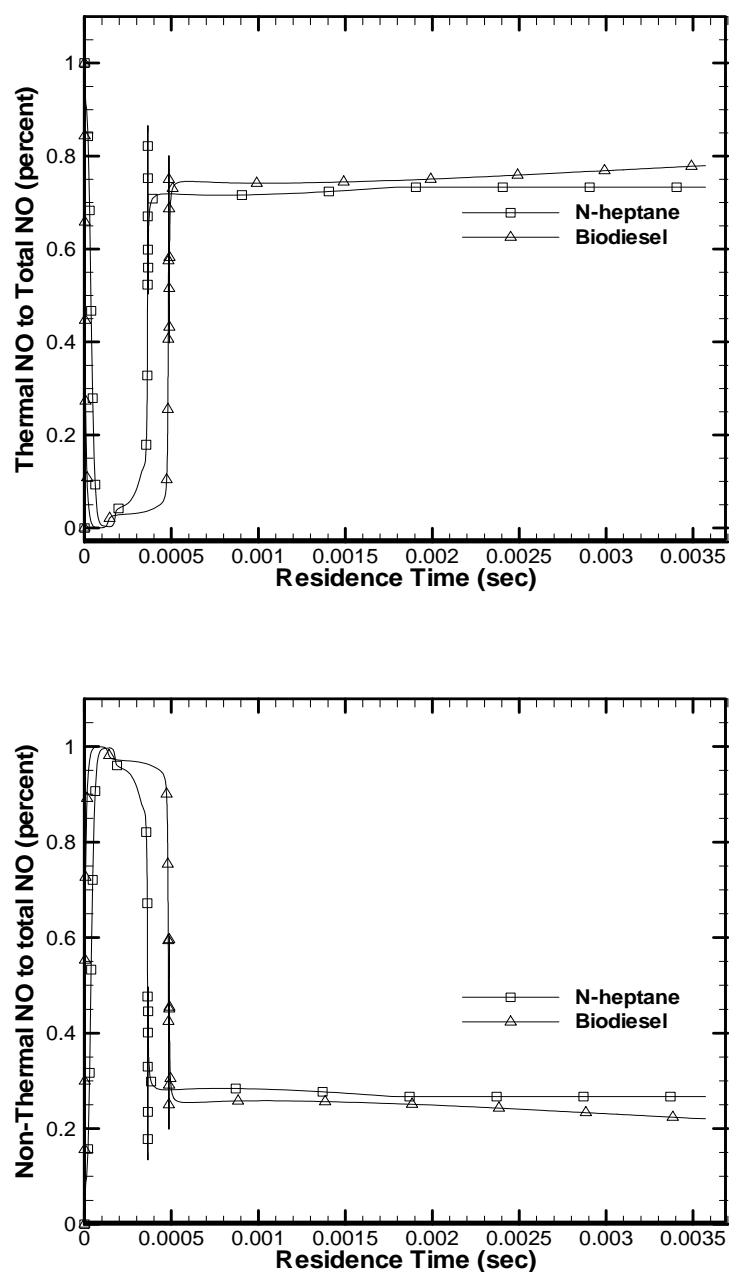


Fig. 7. Computed thermal NO and non-thermal NO contribution to total NO as a function of reactor residence time in a zero-dimensional constant pressure homogeneous reactor at initial temperature and pressure of 886 K and 60 bars respectively for n-heptane and the biodiesel surrogate.

The trends for concentrations of oxygen and temperature are analyzed next as a function of residence reactor time to determine the relationship between oxygen in the fuel-air mixture and the thermal NO for the biodiesel surrogate and the n-heptane. This is done because thermal NO is the dominant contributor to total NO formation for the two fuel surrogates, and oxygen in the fuel-air mixture influences the mixture temperature and therefore the formation of thermal NO. These trends are shown in Fig. 8. As seen in Fig. 8, the oxygen in the biodiesel-air mixture decreased drastically a few microseconds after the n-heptane did during combustion and leveled off to a concentration higher than the n-heptane. Consequently, the temperature of the biodiesel-air mixture increased drastically a few microseconds after the n-heptane did during combustion and leveled off to a temperature lower than the n-heptane. These trends show that the biodiesel consumes the same percentage of oxygen in the fuel-air mixture less efficiently than the n-heptane. Moreover, the biodiesel surrogate uses a lower amount of oxygen than the n-heptane during combustion.

Since the experimental conditions between the fuel surrogates are the same and the only difference between the two surrogates is the addition of methyl esters (fuel-bound oxygen molecules) to the n-heptane (to form biodiesel), the slow decomposition of methyl esters into species which may interact with the oxygen in the fuel-air mixture was supposed to result in low oxygen consumption efficiency for the biodiesel. Fig. 9, however, shows that both the methyl esters and the n-heptane in the biodiesel surrogate are consumed less efficiently than the n-heptane. Hence, a combination of delay in consumption of the n-heptane and the methyl esters may result in lower oxygen

consumption (the horizontal shift in trends for temperature and oxygen concentrations, seen in Fig. 8) for the biodiesel surrogate relative to the n-heptane. Interestingly, the methyl esters in the biodiesel surrogate blend are consumed more efficiently than the n-heptane in the biodiesel surrogate. This result indicates that the fuel-bound oxygen in the methyl esters may play a favorable role in biodiesel combustion. The lower utilization of oxygen for biodiesel relative to the n-heptane could not be explained, but is perhaps bec-

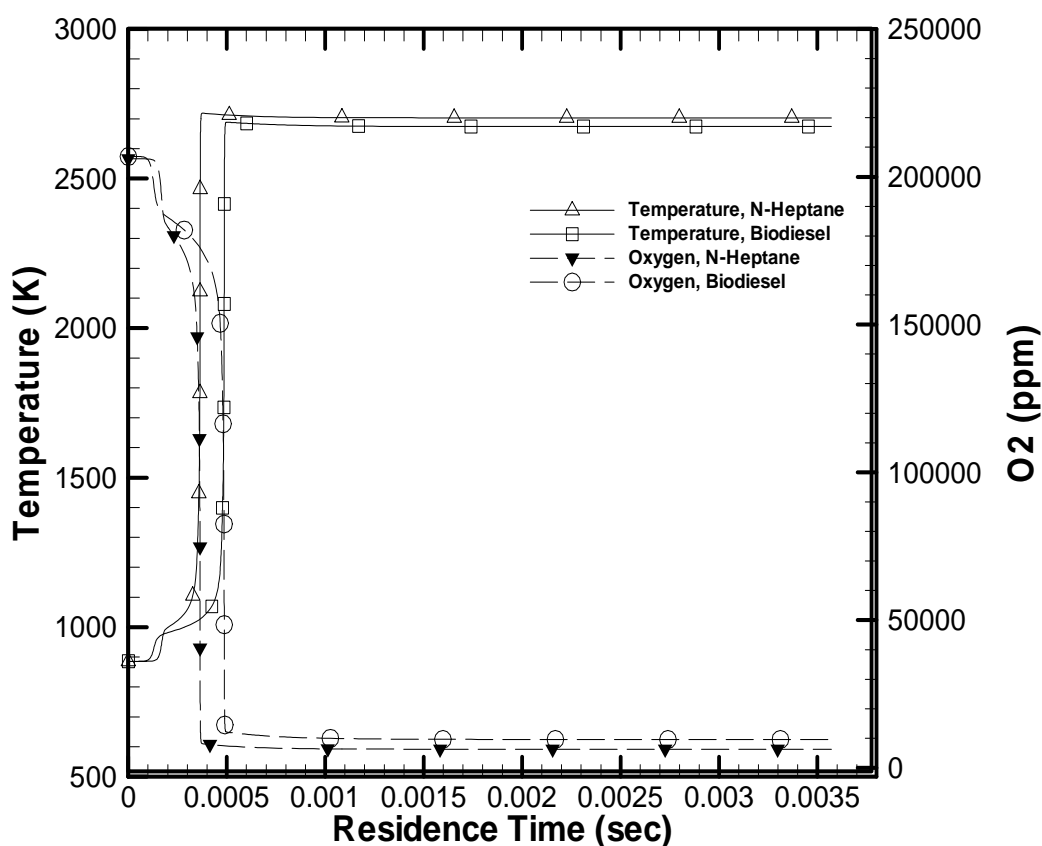


Fig. 8. Computed temperature and oxygen as a function of reactor residence time in a zero-dimensional constant pressure homogeneous reactor at initial temperature and pressure of 886 K and 60 bars respectively for n-heptane and the biodiesel surrogate.

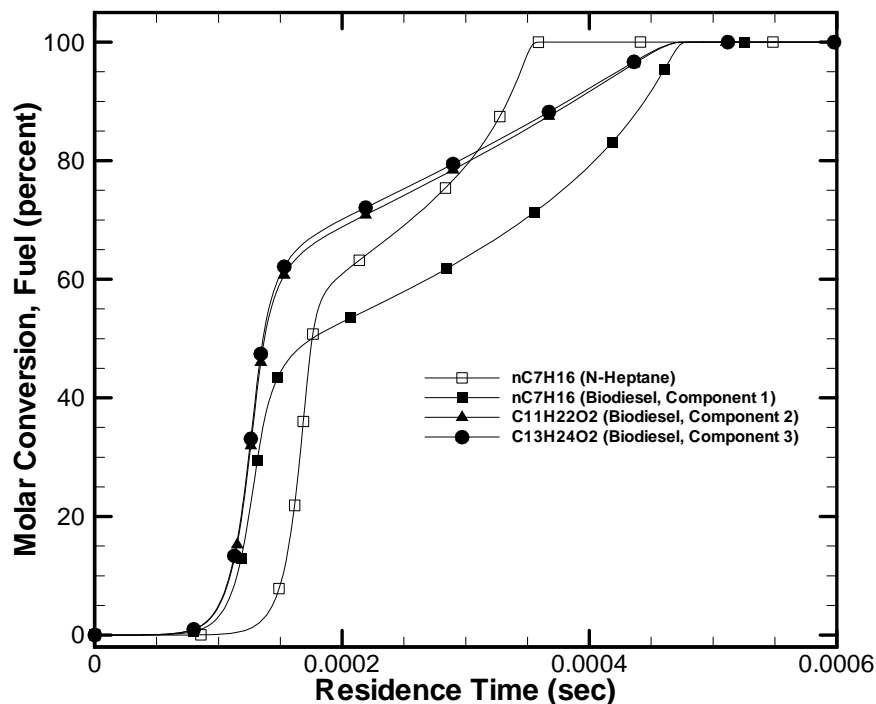


Fig. 9. Molar fuel conversion as a function of reactor residence time in a zero-dimensional constant pressure homogeneous reactor at initial temperature and pressure of 886 K and 60 bars respectively for n-heptane and the fuel components of the biodiesel surrogate.

-ause of the relative mole fractions of components in the biodiesel surrogate. This conclusion however should be validated via an analysis similar to one in Mueller et al.'s study [18]. Regardless, as seen from Fig. 8 and Fig. 6, the delay in temperature rise for the biodiesel surrogate is consistent with the delay in NO_x formation rise for the biodiesel surrogate. The combination of high post-flame gas temperature and high oxygen availability in the biodiesel surrogate-air mixture results in higher NO_x formation

for the biodiesel surrogate relative to the n-heptane. Ultimately, the low oxygen consumption efficiency of the biodiesel surrogate yields higher NO_x concentrations than the n-heptane at the same oxygen equivalence ratio.

Additionally, the relative NO formation pathways at similar NO (ppmvd) values are analyzed to identify the differences between dominant NO formation pathways for the biodiesel surrogate and the n-heptane. Table 3 shows the total rate of production of NO at 2000, 4000, and 6000 ppmvd for both the biodiesel surrogate and the n-heptane. Fig. 10-13 show the relative magnitudes of the absolute rate of production of NO for the dominant reaction mechanisms at the respective NO (ppmvd) values. As seen from Table 3, the total rate of production of NO for the n-heptane is slightly higher than the biodiesel surrogate at 2000 ppmvd. Conversely, the rate of production of NO for the biodiesel is higher than the n-heptane at 4000 and 6000 ppmvd. An analysis of the relative rates of production of NO (Fig. 10-13) shows that different NO production mechanisms are dominant for the n-heptane and the biodiesel surrogate at the same NO value.

Table 3.

Total rate of production of NO at select NO values for the n-heptane and the biodiesel surrogate.

NO (ppmvd)	Total Rate of Production of NO (mole/cm ³ -sec)	
	N-Heptane	Biodiesel Surrogate
2000 ± 250	4.42E-03	4.01E-03
4000 ± 142	2.50E-03	2.52E-03
6000 ± 48	2.41E-05	9.06E-04

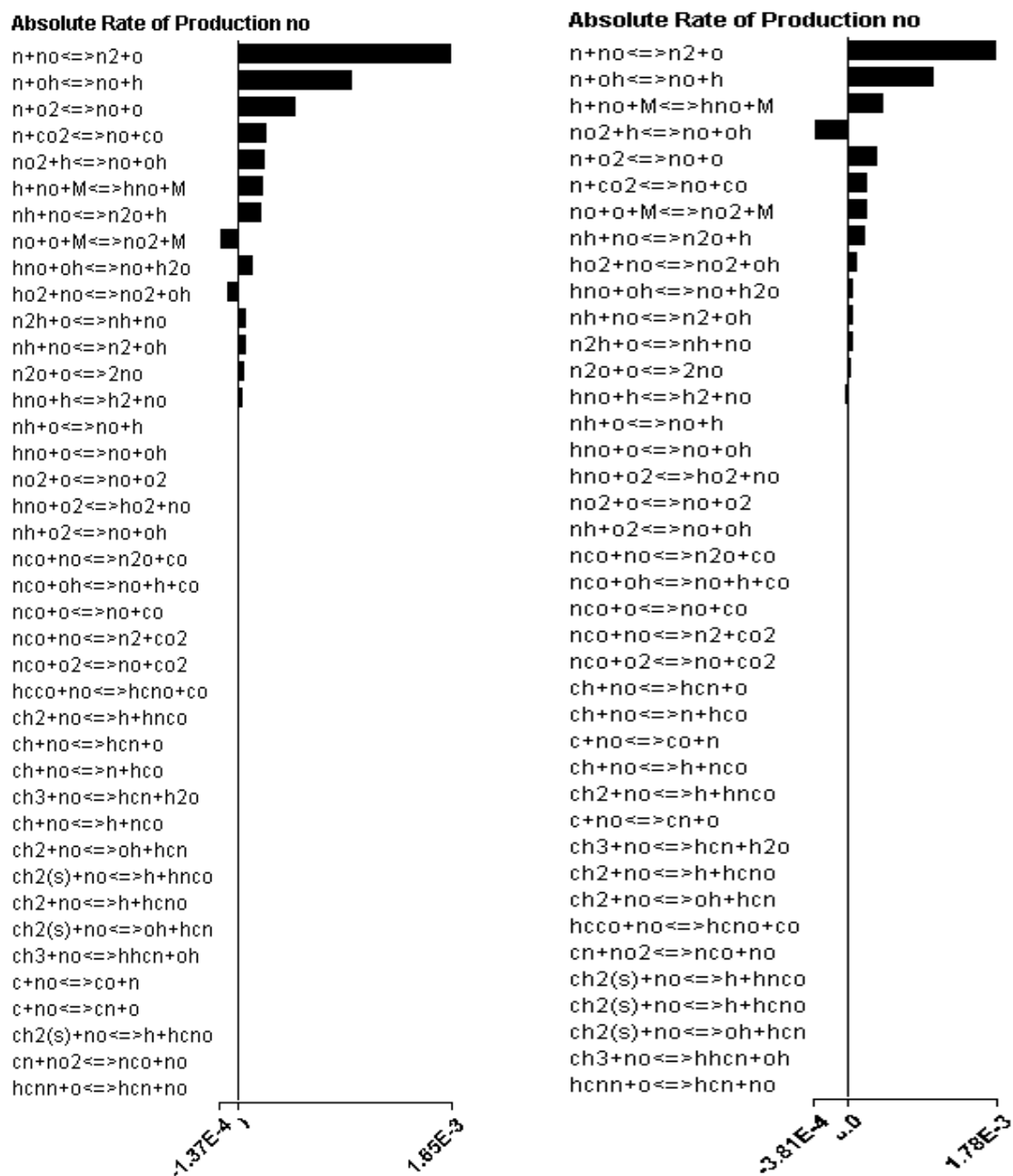


Fig. 10. Absolute rate of production of NO for the dominant NO formation mechanisms at nominal 2000 ppmvd. Biodiesel (left). N-Heptane (right).

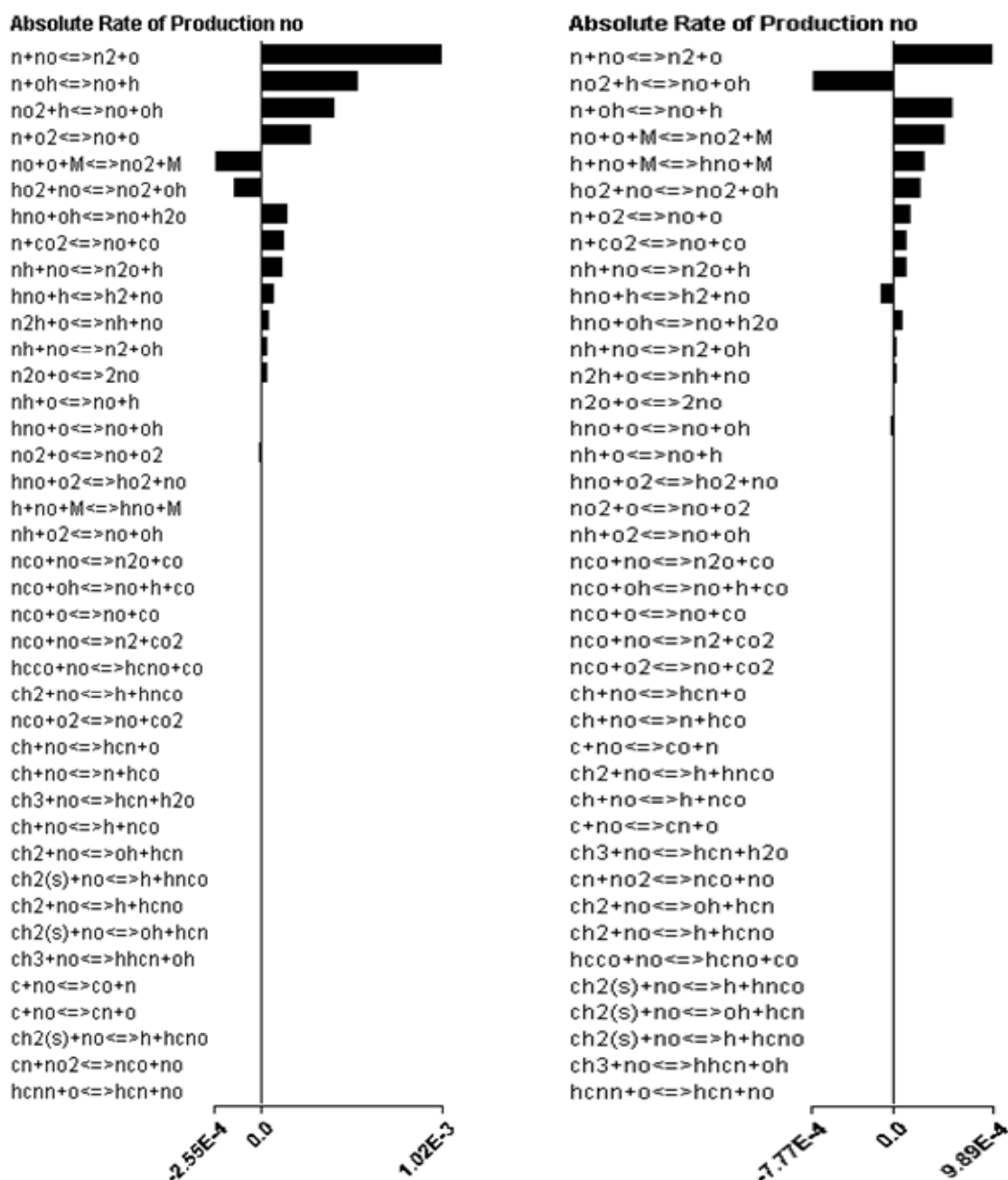


Fig. 11. Absolute rate of production of NO for the dominant NO formation mechanisms at nominal 4000 ppmvd. Biodiesel (left). N-Heptane (right).

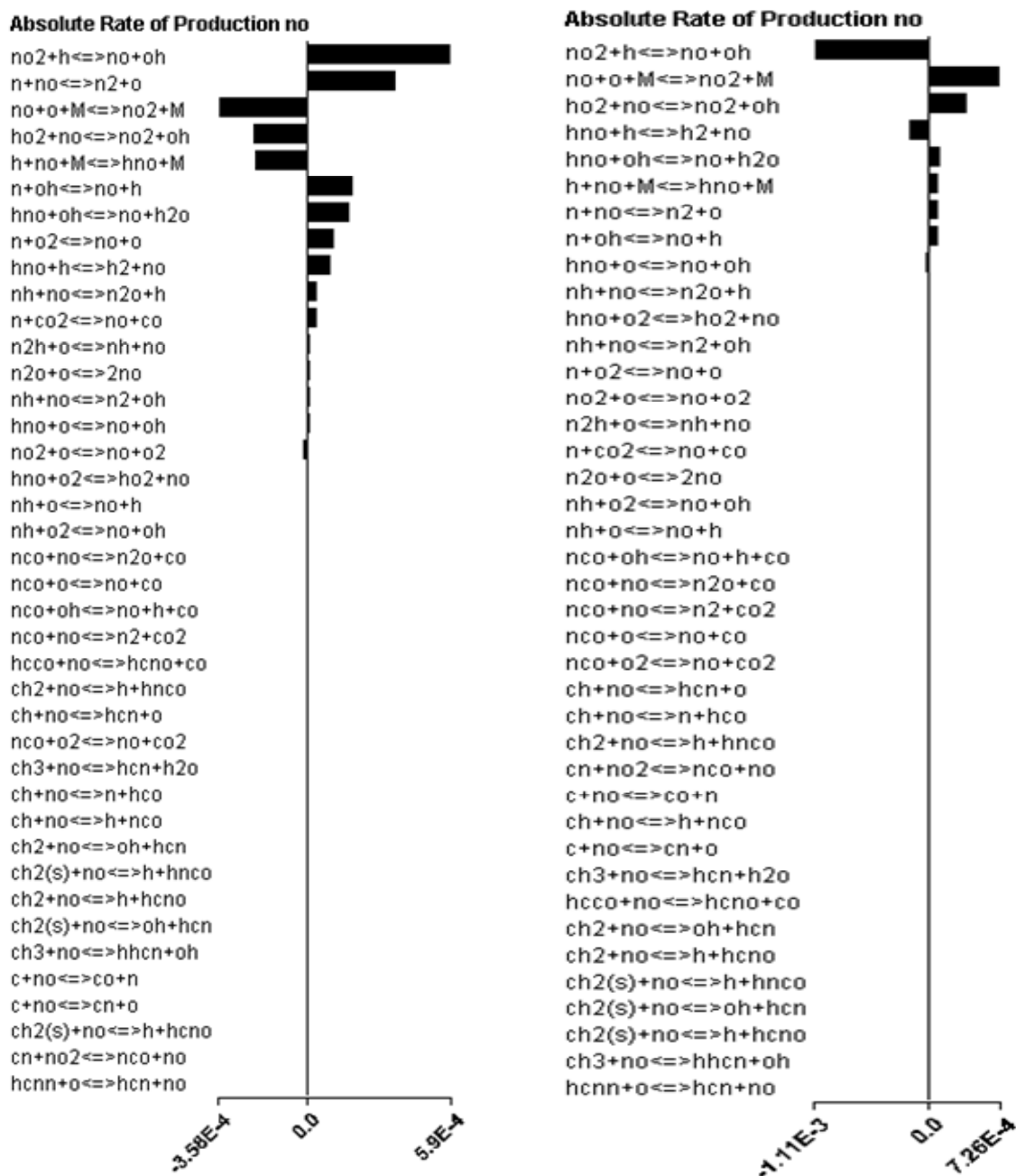


Fig. 12. Absolute rate of production of NO for the dominant NO formation mechanisms at nominal 6000 ppmvd. Biodiesel (left). N-Heptane (right).

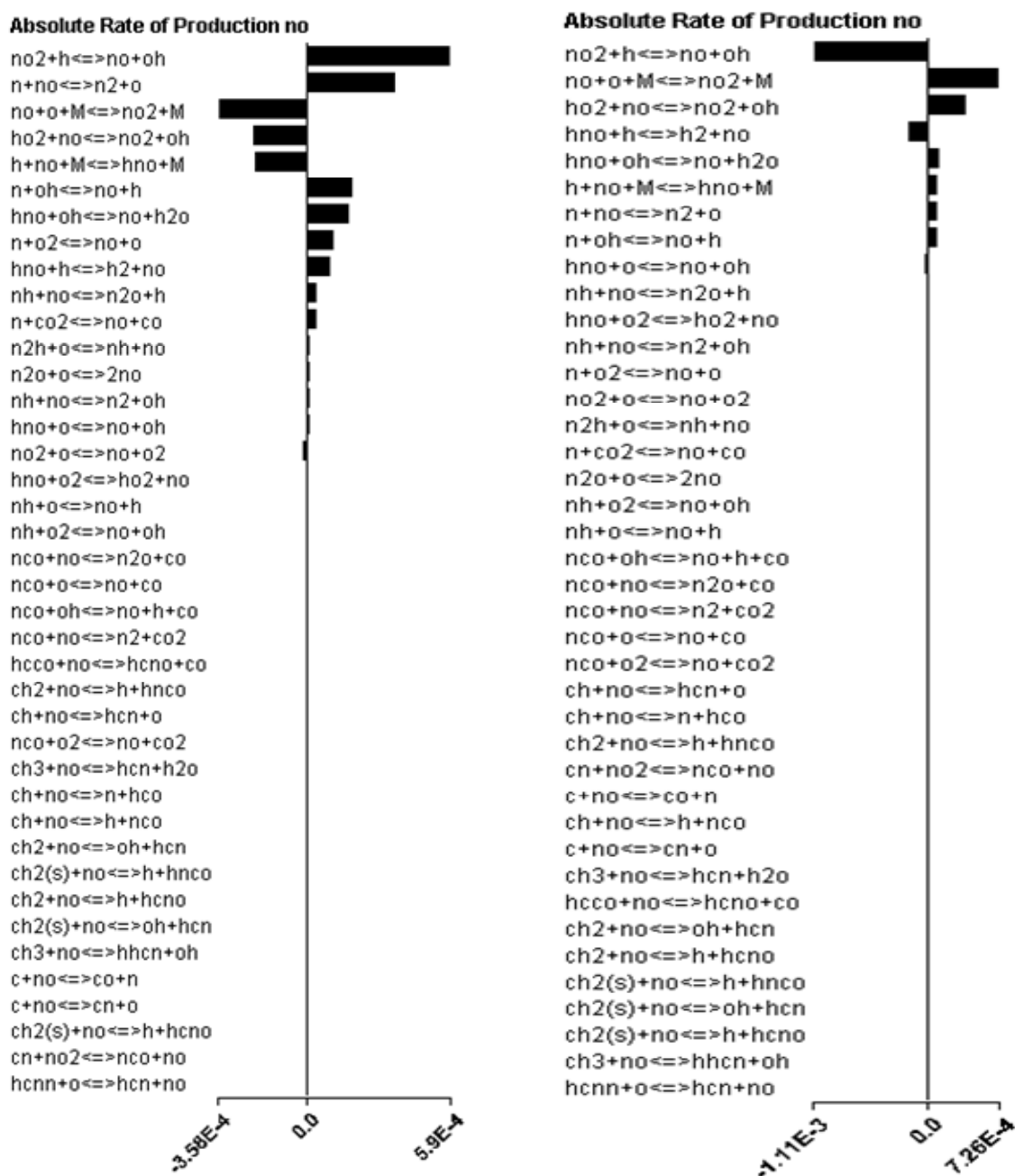


Fig. 13. Absolute rate of production of NO for the dominant NO formation mechanisms at reactor residence time of 0.003571 seconds. Biodiesel (left). N-Heptane (right).

The thermal mechanisms for the n-heptane are more dominant than the biodiesel surrogate at 2000 ppmvd. This results in higher rates of formation of NO for the n-heptane at 2000 ppmvd. Conversely, the thermal NO formation mechanisms for the biodiesel surrogate are active and more dominant than the n-heptane at 4000 ppmvd. This results in higher rates of formation of NO for the biodiesel at 4000 ppmvd. The $\text{NO}_2 + \text{H} \leftrightarrow \text{NO} + \text{OH}$ and $\text{N} + \text{NO} \leftrightarrow \text{N}_2 + \text{O}$ mechanisms appear to be the dominant NO production pathways at 6000 ppmvd and 0.003571 for the biodiesel surrogate. On the other hand, the lower rate of formation of NO for the n-heptane at 4000 and 6000 ppmvd and 0.003571 seconds results from destruction of NO mainly via the $\text{NO}_2 + \text{H} \leftrightarrow \text{NO} + \text{OH}$ mechanism. It appears that if the $\text{NO}_2 + \text{H} \leftrightarrow \text{NO} + \text{OH}$ and $\text{N} + \text{NO} \leftrightarrow \text{N}_2 + \text{O}$ mechanisms are suppressed for the biodiesel, the biodiesel could produce lower NO emissions than the petroleum diesel.

3.3 Limitations and Recommendations

The objective of this study was accomplished within the modeling capabilities of CHEMKIN PRO. Even though the role of fuel-bound oxygen in biodiesel on increases in NO emissions could not be isolated in the current study, some conclusions (as described in section 3.2) have been drawn on the role of oxygen in the biodiesel surrogate fuel-air mixture on NO emissions increases for biodiesel relative to the n-heptane. These conclusions however can be further verified and validated experimentally. Therefore, the following improvements are suggested to overcome limitations of the current work:

1. *Limitation # 1, Verification of the 0-D Homogeneous Reactor:* The 0-D constant pressure homogeneous model could not be completely verified with the EQUIL reactor for the biodiesel surrogate because the process is computationally expensive.

Recommendation: The computational expense to verify the 0-D homogeneous model can be minimized by reducing the number of detailed mechanisms in the biodiesel surrogate file. This can be done by removing one species (and the corresponding reactions) at a time from the original file, and using the truncated mechanisms file to check if the global behavior of the fuel surrogate is maintained relative to experimental conditions for the initial conditions of the current study. Given the number of species and reactions in the biodiesel surrogate mechanisms file, this however is a daunting task.

2. *Limitation # 2, Characterization of Error in the Solution:* The error bars for the temperature, and concentrations of NO and oxygen have not been determined for the fuel surrogates. This calculation is essential to conclude that the computed differences between the temperatures and concentrations of NO and oxygen for the fuel surrogates are significant.

Recommendation: The uncertainty in the computation of temperatures and concentrations of NO and oxygen is introduced via the uncertainty associated with experimentally determined reaction rate constant values for the reaction mechanisms. An uncertainty analysis on the reaction rate constants for the dominant NO formation reactions can be run to determine the error bars for the

calculations in the current study. This analysis will aid in verifying the significance of the current conclusions.

3. *Limitation # 3, Validation of Conclusions in a Diesel Engine:* The conclusions of current study have been derived under idealized diesel engine conditions. Moreover, though modeled using experimentally validated reaction mechanisms, the conclusions of the current study have not been experimentally validated.

Recommendation: The multi-zone engine model in CHEMKIN PRO can be used to realistically model diesel engine combustion. Moreover, the model can be experimentally validated to check the veracity of the conclusions from the current study.

4. *Limitation # 4, Explanation for the Low Utilization of Oxygen in the Biodiesel Surrogate-Air Mixture and the Role of Fuel-bound Oxygen in Biodiesel on Increases in NO Emissions:* The reasons behind the lower oxygen consumption efficiency for the biodiesel surrogate could be reinforced with supporting evidence. Moreover, evidence ought to be collected to explain the role of fuel-bound oxygen in biodiesel on NO emissions increases for biodiesel relative to petroleum diesel.

Recommendation: An analysis similar to the one in Muller *et al.* [18] may be conducted in CHEMKIN PRO to determine how the fuel-bound oxygen or the oxygen in the fuel-air mixture is being utilized during combustion for the biodiesel surrogate.

4. SUMMARY AND CONCLUSIONS

4.1 Summary

Interest in biodiesel fuels has piqued with the advent of fossil fuel depletion and stringent emissions regulations. Biodiesel is a viable substitute for petroleum diesel because biodiesel produces significantly lower particulate and soot emissions relative to petroleum diesel. Higher NO emissions for biodiesel relative to petroleum diesel, however, are of primary concern in light of the stringent emissions regulations. This observed increase in NO emissions has motivated the current research on improving our understanding of fundamental factors that drive an increase in NO emissions for biodiesel compared to petroleum diesel. The potential factors that may increase NO formation for biodiesel are fuel-bound oxygen, fuel-bound nitrogen and the post-flame gas temperature. The role of fuel-bound oxygen content, however, is debated in the literature. Hence, the effect of fuel-bound oxygen content in biodiesel on increased NO emissions has been investigated for biodiesel relative to petroleum diesel.

The research objective of this study is to computationally determine if biodiesel and petroleum diesel yield equivalent NO concentrations with the same oxygen equivalence ratio in a 0-D homogeneous reactor, to explain the role of fuel-bound oxygen in biodiesel on increases in NO emissions with biodiesel. While several researchers have previously investigated the emissions reduction effectiveness of oxygenated and non-oxygenated fuels under a comparable environment, there is no consensus in the literature on the effect of equivalent oxygenation on NO_x emissions

between the oxygenated and non-oxygenated fuels. This is partially because the researchers have not used a comparable measure to quantify the oxygen in the fuel-air mixture. Only one researcher has isolated the effect of fuel-bound oxygen on NO_x emissions; his study, however, compares ether blends to petroleum diesel. Biodiesel is a long chain methyl ester. This study is significant because it is the first documentation (to the author's knowledge) of a comparative study between biodiesel and petroleum diesel under comparable oxygen environment (using the oxygen equivalence ratio), to provide insight into the role of fuel-bound oxygen in biodiesel on increases in NO emissions for biodiesel relative to petroleum diesel.

A numerical simulation in a zero-dimensional (0-D) constant pressure homogeneous reactor is conducted at the same oxygen equivalence ratio using a biodiesel surrogate blend and n-heptane to model biodiesel and petroleum diesel respectively in CHEMKIN PRO. The reaction mechanisms for the biodiesel surrogate and the n-heptane are obtained from the literature. The oxygen equivalence ratio is selected for comparison because it is considered a more accurate measure of mixture stoichiometry than the traditional equivalence ratio, the oxygen to carbon ratio, and the oxygen mass fraction. The initial temperature, pressure and reactor residence time are set to 886 K, 60 bars and 3.571 milliseconds. The equivalence ratio is computed from the oxygen equivalence ratio and set to 1.0. The initial mole fractions are computed and set to 1.0 for the n-heptane, 0.3333 each for the biodiesel surrogate blend components, 0.2100 for the oxygen and 0.7899 for the nitrogen for the stoichiometric reactions. Before the temperature, the concentrations of NO_x and oxygen, the molar fuel conversion

percent, and the absolute rate of production of dominant NO formation pathways are collected from the 0-D constant pressure homogeneous reactor for the two surrogate fuels, the 0-D homogeneous reactor is verified against the equilibrium reactor in CHEMKIN PRO. The equilibrium reactor in turn is verified against an independent program, the Adiabatic Flame Temperature Program. A summary of the findings is provided below:

1. The combustion temperatures and concentrations of NO_x and oxygen from the EQUIL model reasonably match the combustion temperatures and concentrations of NO_x from the 0-D constant pressure homogeneous reactor for both the biodiesel surrogate and the n-heptane.
2. The biodiesel surrogate yields higher NO_x concentrations than the n-heptane at the same oxygen equivalence ratio (i.e. the same percentage of oxygen).
3. The thermal NO is a major contributor to total NO formation for both the biodiesel surrogate and the n-heptane. The thermal NO concentration for the biodiesel surrogate however is higher than the n-heptane at the end of combustion.
4. The non-thermal NO concentration is lower for the biodiesel surrogate than the n-heptane close to the end of combustion.
5. The temperature for the n-heptane is higher than the biodiesel surrogate at the end of combustion. A delay in temperature rise (relative to the n-heptane) is observed for the biodiesel surrogate.

6. The oxygen in the biodiesel surrogate-air mixture is consumed less efficiently than the n-heptane, and higher percentage of oxygen (relative to the n-heptane) is observed for the biodiesel surrogate at the end of combustion.
7. The surrogate biodiesel fuel components (n-heptane and methyl esters) convert to products less efficiently than the n-heptane. The methyl esters in the biodiesel surrogate burn more efficiently than the n-heptane in the biodiesel surrogate.
8. $\text{NO}_2 + \text{H} \leftrightarrow \text{NO} + \text{OH}$ and $\text{N} + \text{NO} \leftrightarrow \text{N}_2 + \text{O}$ are the dominant NO formation mechanisms for the biodiesel surrogate at nominal 6000 ppmvd (point where the NO concentration of the biodiesel surrogate has already surpassed the n-heptane) and 0.003571 seconds (time at which the species leave the reactor). $\text{NO}_2 + \text{H} \leftrightarrow \text{NO} + \text{OH}$ is the dominant NO destruction mechanism for the n-heptane at the same concentration and residence time.

Additionally, the need to verify the 0-D homogeneous reactor for the biodiesel surrogate, to characterize the error in the numerical solution, and to further validate our conclusions under diesel engine conditions has been identified and recommendations to improve upon these limitations have also been suggested in this work.

4.2 Conclusions

The objective of this study is accomplished within the modeling capabilities of CHEMKIN PRO. Even though the role of fuel-bound oxygen in biodiesel on increases in NO emissions could not be isolated in the current study, some conclusions have been drawn on the role of oxygen in the biodiesel surrogate fuel-air mixture on NO emissions

increases for the biodiesel relative to the n-heptane in a 0-D homogeneous reactor. The results from this study indicate that the biodiesel surrogate yields higher NO emissions than the n-heptane because of lower oxygen consumption efficiency than the n-heptane. The error in the computed oxygen concentrations however should be characterized via an uncertainty analysis on the reaction rate constants to determine the significance of computed differences in the oxygen consumption efficiency for the two surrogate fuels. If significant, the lower oxygen consumption efficiency for biodiesel is likely because of the slower decomposition of the individual components and the blending ratios of the biodiesel surrogate blend. The relative differences in combustion efficiency of individual components of the biodiesel blend suggest this conclusion. The more efficient burning of the methyl esters relative to the n-heptane in the biodiesel surrogate perhaps indicates the favorable role of fuel-bound oxygen in the fuel's combustion. The low utilization of oxygen by the biodiesel surrogate however could not be explained in the current study. The dominance of $\text{NO}_2 + \text{H} \leftrightarrow \text{NO} + \text{OH}$ and $\text{N} + \text{NO} \leftrightarrow \text{N}_2 + \text{O}$ mechanisms during biodiesel combustion explains the high NO emissions for the biodiesel surrogate relative to the n-heptane. The biodiesel may yield the same or lower NO emissions than the petroleum diesel if the blending ratios of the components in the biodiesel are adjusted such that combustion efficiency is the same for both biodiesel and petroleum diesel and the $\text{NO}_2 + \text{H} \leftrightarrow \text{NO} + \text{OH}$ and $\text{N} + \text{NO} \leftrightarrow \text{N}_2 + \text{O}$ mechanisms are suppressed during biodiesel combustion. These conclusions however are derived from results in a zero-dimensional reactor under idealized conditions, and therefore, their universality and

application to a diesel engine should be verified in a multi-zone reactor in CHEMKIN PRO and validated experimentally in a diesel engine.

REFERENCES

- [1] A.K. Agarwal, Prog. Energy Combust. Sci. 33 (2007) 233-271.
- [2] A. Demirbas, Prog. Energy Combust. Sci. 33 (2007) 1-18.
- [3] C.D. Rakopoulos, D.T. Hountalas, T.C. Zannis, Y.A. Leventis, T SAE J. Fuels Lubr. 113 (2004) 1723-1743.
- [4] C.T. Bowman, Prog. Energy Combust. Sci. 1 (1975) 33-45.
- [5] J. Sun, J.A. Caton, T.J. Jacobs, Prog. Energy Combust. Sci. (2010), DOI: 10.1016/j.pecs.2010.02.004.
- [6] M. Lapuerta, O. Armas, J. Rodriguez-Fernandez, Prog. Energy Combust. Sci. (2007), DOI: 10.1016/j.pecs.2007.07.001.
- [7] M.S. Graboski, R.L. McCormick, Prog. Energy Combust. Sci. 24 (1998) 125-164.
- [8] H.C. Watson, E. Gaynor, G.R. Rigby, Oxygen Enrichment: a Method for Reduced Environmental Impact and Improved Economics, Institution of Mechanical Engineers, London, U.K., 1990.
- [9] J. Ghojel, J.C. Hilliard, J.A. Leventis, Effect of Oxygen Enrichment on the Performance and Emissions of I.D.I Diesel Engines, SAE International, Warrendale, Pennsylvania, USA, 1983.
- [10] K.S. Virk, U. Kopturk, C.R. Bartles, Effects of Oxygen-Enriched Air on Diesel Engine Exhaust Emissions and Engine Performance, SAE International, Warrendale, Pennsylvania, USA, 1993.
- [11] D.N. Assanis, R.B. Poola, R. Sekar, G.R. Cataldi, J. Eng. Gas Turb. Power 123 (1) (2001) 157-166.
- [12] R.B. Poola, R. Sekar, J. Eng. Gas Turb. Power 125 (2) (2003) 524-533.
- [13] M. Lapuerta, O. Armas, R. Ballesteros, Diesel Particulate Emissions from Biofuels Derived from Spanish Vegetable Oils, SAE International, Warrendale, Pennsylvania, USA, 2002.
- [14] M. Canakci, Proc. I MECH E Part D J. Automob. Eng. (2005) D7:915-922.

- [15] W. Yuan, A.C. Hansen, M.E. Tat, J.H. Van Gerpen, Z. Tan, T ASAE 48 (3) (2005) 933-939.
- [16] T.C. Zannis, E.G. Pariotis, D.T. Hountalas, D.C. Rakopoulos, Y.A. Levendis, *Energ. Convers. Manage.* 48 (11) (2007) 2962-2970.
- [17] J. Song, V. Zello, A.L. Boehman, F.J. Waller, *Energy and Fuels* 18 (5) (2004) 1282-1290.
- [18] C. J. Mueller, W.J. Pitz, L.M. Pickett, G.C. Martin, D.L. Siebers, C.K. Westbrook, T SAE J. Fuels Lubr. 112 (2003) 964-981.
- [19] R.J. Donahue, D.E. Foster, T SAE J. Fuels Lubr. 109 (2000) 334-349.
- [20] CHEMKIN-PRO 15092, Reaction Design: San Diego, 2009.
- [21] O. Herbinet, W.J. Pitz, C.K. Westbrook, *Combust. Flame* (2010), <http://dx.doi.org/10.1016/j.combustflame.2009.10.013> LLNL-JRNL-414930 23 June 2010.
- [22] H.J. Curran, P. Gaffuri, W.J. Pitz, C.K. Westbrook, *Combust. Flame* (1998) 114:149-177.
- [23] G.P. Smith, D.M. Golden, M. Frenklach, N.W. Moriarty, B. Eiteneer, M. Goldenberg, C.T. Bowman, R.K. Hanson, S. Song, W.C. Gardiner, Jr., V.V. Lissianski, Z. Qin GRI-Mech 3.0 from http://www.me.berkeley.edu/gri_mech/ 23 June 2010.
- [24] A. Burcat, B. Ruscic, Third Millennium Ideal Gas and Condensed Phase Thermochemical Database for Combustion with updates from Active Thermochemical Tables, ANL-05/20 and TAE 960 Technion-IIT, Aerospace Engineering, and Argonne National Laboratory, Chemistry Division, September 2005.
- [25] C.J. Mueller, The Quantification of Mixture Stoichiometry When Fuel Molecules Contain Oxidizer Elements or Oxidizer Molecules Contain Fuel Elements, SAE International, Warrendale, Pennsylvania, USA, 2005.

VITA

Name: Gurlovleen K. Rathore

Address: 218 Thompson Hall
Advanced Engine Research Lab
Texas A&M University
Mail Stop: 3123
College Station, TX 77843

Email Address: fiza@tamu.edu

Education: B.S., Engineering Physics, University of Michigan, 2007
M.S., Mechanical Engineering, Texas A&M University, 2010